

MODELING AND ANALYSIS OF ENSEMBLE AVERAGE SOLVATION ENERGY AND SOLUTE-SOLVENT INTERFACIAL FLUCTUATIONS

YUANZHEN SHAO^{*†}, ZHAN CHEN^{**}, AND SHAN ZHAO^{***}

ABSTRACT. Variational implicit solvation models (VISM) have gained extensive popularity in the molecular-level solvation analysis of biological systems due to their cost-effectiveness and satisfactory accuracy. Central in the construction of VISM is an interface separating the solute and the solvent. However, traditional sharp-interface VISM fall short in adequately representing the inherent randomness of the solute-solvent interface, a consequence of thermodynamic fluctuations within the solute-solvent system. Given that experimentally observable quantities are ensemble-averaged, the computation of the ensemble average solvation energy (EASE)-the averaged solvation energy across all thermodynamic microscopic states-emerges as a key metric for reflecting thermodynamic fluctuations during solvation processes. This study introduces a novel approach to calculating the EASE. We devise two diffuse-interface VISM: one within the classic Poisson-Boltzmann (PB) framework and another within the framework of size-modified PB theory, accounting for the finite-size effects. The construction of these models relies on a new diffuse interface definition $u(x)$, which represents the probability of a point x found in the solute phase among all microstates. Drawing upon principles of statistical mechanics and geometric measure theory, we rigorously demonstrate that the proposed models effectively capture EASE during the solvation process. Moreover, preliminary analyses indicate that the size-modified EASE functional surpasses its counterpart based on classic PB theory across various analytic aspects. Our work is the first step towards calculating EASE through the utilization of diffuse-interface VISM.

1. INTRODUCTION

In the quantitative analysis of biological processes, the complex interactions between the solute and solvent are typically described by solvation energies (or closely related quantities): the free energy of transferring the solute (e.g. biomolecules, such as proteins, DNA, RNA) from the vacuum to a solvent environment of interest (e.g. water at a certain ionic strength). There are two major approaches for solvation energy calculations: explicit solvent models and implicit solvent models [40]. Explicit models, treating both the solute and the solvent as individual molecules, are too computationally expensive for large solute-solvent systems, such as the solvation of macromolecules in ionic environments. In contrast, implicit models, by averaging the effect of solvent phase as continuum media [1, 2, 8, 9, 11, 25, 39], are much more efficient and thus are able to handle much larger systems [2, 15, 27, 29, 30, 35, 42, 47].

An inevitable prerequisite for describing the solvation energy in implicit solvent models is an interface separating the discrete solute and the continuum solvent domains. All of the physical properties related to solvation processes, including biomolecular surface area, biomolecular cavitation volume, pK_a value and electrostatic free energy, are very sensitive to the interface definition [20, 46, 48]. There are a number of different surface definitions, which include the van der Waals surface, the solvent excluded surface and the solvent accessible surface. These surface definitions have found many successful applications in biomolecular modeling [18, 21, 34, 45]. However, these predetermined interfaces are *ad hoc* partitions and thus either non-negligibly overestimate or underestimate the solvation free energies [48]. Moreover, none of them takes into account the minimization of interfacial free energies during the equilibrium solvation.

Variational implicit solvation models (VISM) stand out as a successful approach to compute the disposition of an interface separating the solute and the solvent [4, 12, 13, 16, 19, 52, 55]. In a VISM, the desired interface

2020 *Mathematics Subject Classification.* Primary: 49Q10; Secondary: 35J20; 92C40.

Key words and phrases. Biomolecule solvation, Poisson-Boltzmann, Variational implicit solvation model, Ensemble average solvation energy, Finite size effect.

[†]Corresponding author.

^{*}Department of Mathematics, The University of Alabama, Tuscaloosa, AL, USA. yshao8@ua.edu.

^{**}Department of Mathematical Sciences, Georgia Southern University, GA, USA. zchen@georgiasouthern.edu.

^{***}Department of Mathematics, The University of Alabama, Tuscaloosa, AL, USA. szhao@ua.edu.

profile is obtained by optimizing a solvation energy functional coupling the discrete description of the solute and the continuum description of the solvent in addition to polar and non-polar interactions.

However, traditional sharp-interface VISM models have limitations in capturing the inherent randomness of the solute-solvent boundary. This randomness arises from factors such as atomic vibrations and thermodynamic fluctuations. In practical applications, ions, solutes, and solvent molecules are not rigid entities; they undergo small or significant conformational changes. The disposition of the solute-solvent interface is influenced by both the structure of the solute molecule and the surrounding solvent configuration. Due to thermodynamic fluctuations, when a fixed solute molecular structure is being considered, solvent molecules and ions can still adopt different configurations [3], equivalent to forming different microstates in the language of statistical mechanics. This highlights that the position of the solute-solvent interface is not unique, and a single, fixed configuration does not capture the full range of possible solute-solvent interactions.

On the other hand, experimentally observable quantities are ensemble averaged. Utilizing the energy computed from a single microstate to predict the averaged energy from all microstates is inherently prone to inaccuracy. Indeed, studies show that disregarding thermodynamic fluctuations during the solvation process can cause severe errors in predictions of solvation free energies [41]. Therefore, it is of imminent practical importance to develop a solvation model capable of calculating ensemble average solvation energy (EASE) with thermodynamic fluctuations being taken into account.

According to statistical mechanics, the ensemble average of a quantity is the weighted average (by means of the Boltzmann weight) of its values among all microstates. However, in practice, it is a challenging task to directly compute the EASE of a solute-solvent system by means of this definition. If one only samples a handful of random realizations, it is likely that one can only capture an outlier behavior rather than the meaningful average behavior of the stochastic regime. In contrast, a tremendous sampling of random realizations, although delivers a more accurate approximation of EASE, is computationally too expensive, sometimes even unaffordable.

To address this dilemma, we provide an alternative approach to the computation of EASE in Section 3. More precisely, we show that instead of computing and averaging the solvation energies among all microstates, one should characterize the “mean behavior” of the solute-solvent interfaces. This gives rise to a novel “interface” profile $u : \Omega \rightarrow [0, 1]$ such that $u(x)$ represents the probability of a point $x \in \Omega$ found in the solute phase among all microstates.

Based on this insight, we rigorously demonstrate that the EASE of a solute-solvent system can be effectively captured by using a VISM defined in terms of this “interface” profile u . This modeling paradigm is highly flexible, enabling us to incorporate various considerations into EASE modeling.

As an illustrative example, we develop two EASE functionals, one within the framework of classic Poisson-Boltzmann (PB) theory and the other within the size-modified PB theory framework to account for finite size effects. These proposed models have the potential to significantly expedite the computation of EASE. They achieve this by using a single diffuse-interface profile instead of numerous sharp interfaces in various microstates, making the computation more efficient and computationally accessible.

The proposed models introduced in this work fall within the category of diffuse-interface VISM [13, 19, 22, 38, 49–51, 53, 54]. This family of models replaces the traditional sharp solute-solvent interface with a diffuse-interface profile, denoted as $u : \Omega \rightarrow \mathbb{R}$. Notably, our EASE models, as described in (3.1.3) and (3.2), have strong connections with one of the most widely employed diffuse-interface VISM models, the Geometric Flow-Based VISM (GFBVISM) [13, 22, 49–51, 53].

Furthermore, our work can be viewed as an enhancement of GFBVISM in several crucial aspects.

First, our research provides a rigorous mathematical foundation for the physical interpretation of the diffuse-interface profile u and the energy predictions generated by our models and GFBVISM. This clarification establishes a link between the sharp-interface and diffuse-interface VISM models, demonstrating that the diffuse-interface model indeed computes “mean” energies consistent with sharp-interface models.

Secondly, we have incorporated two physical constraints into the formulations of (3.1.3) and (3.2). These constraints effectively eliminate the ill-posed issues associated with GFBVISM and guarantee the optimal diffuse-interface profiles align with the physical principles.

Lastly, our first model, (3.1.3), corrects the formulation of the polar component of GFBVISM, while the second model, (3.2), builds upon this correction by incorporating finite size effects into the model. This results in a more accurate representation of the solvation process, which is a significant improvement over the original GFBVISM formulation.

The rest of this paper is organized as follows. Section 2 provides an introduction to one of the most widely used formulations of sharp-interface VISMs. In Section 3, we present the development of two Ensemble Average Solvation Energy (EASE) functionals within the frameworks of classic Poisson-Boltzmann theory and the size-modified Poisson-Boltzmann theory, taking into account finite size effects. Section 4 comprises preliminary analyses of the proposed EASE models, with a particular emphasis on the size-modified EASE functional. In Appendix A, we gather relevant information and facts about a class of strictly convex functionals related to the polar portion of EASE. Appendix B offers a brief comparative analysis between our newly proposed models and the Geometric Flow-Based Variational Implicit Solvent Model (GFBVISM). Finally, in Section 5, we draw conclusions and summarize the key findings and implications of our research.

2. ENSEMBLE AVERAGED SOLVATION ENERGY

List of Notations: Given any open sets U and Ω , $U \Subset \Omega$ means that $\bar{U} \subset \Omega$ and \bar{U} stands for the closure of U . We denote by \mathcal{L}^N and \mathcal{H}^{N-1} the N -dimensional Lebesgue measure and the $(N-1)$ -dimensional Hausdorff measure, respectively. For any $1 \leq p \leq \infty$, p' is the Hölder conjugate of p . The phrase l.s.c is the abbreviation of lower semi-continuous. χ_E always denotes the characteristic function of a set E . For any two Banach spaces X and Y , the notation $\mathcal{L}(X, Y)$ stands for the set of all bounded linear operators from X to Y and $\mathcal{L}(X) := \mathcal{L}(X, X)$.

2.1. Background. We consider a solute-solvent system with a fixed biomolecular structure contained in a bounded Lipschitz domain $\Omega \subset \mathbb{R}^3$ by using a (statistical) grand canonical ensemble. The temperature, chemical potentials and volume of the system are kept constant. Suppose that there are N_c ion species in Ω and the system contains $N_c + 2$ types of particles, i.e. the solute and solvent molecules and N_c ion species. We assume that the solute atoms are centered at $x_1, \dots, x_{N_m} \in \Omega$.

Define a probability space $(\mathcal{S}, \mathcal{F}, \mathcal{P})$, where the sample space $\mathcal{S} = \{\mathcal{S}_\alpha : \alpha \in A\}$ denotes the set of all possible states of the system with A being the index set of the states. \mathcal{F} is a σ -algebra of \mathcal{S} and \mathcal{P} is the probability measure. Because a biomolecular structure is fixed, each state \mathcal{S}_α is uniquely determined by a function

$$\mathcal{C}_\alpha \in L^1(\Omega; \mathbb{R}^{N_c+1}) : \mathcal{C}_\alpha(x) = (\mathcal{C}_{\alpha,0}(x), \mathcal{C}_{\alpha,1}(x), \dots, \mathcal{C}_{\alpha,N_c}(x)),$$

where $\mathcal{C}_{\alpha,j}(x)$ is the (number) concentration of the j -th ion species at x for $j = 1, \dots, N_c$, or the (number) concentration of solvent molecules for $j = 0$. In state \mathcal{S}_α , a point $x \in \Omega$ is in the solute phase if $\mathcal{C}_\alpha(x) = (0, \dots, 0)$; otherwise in the solvent phase. A point that is not occupied by any particle is typically considered to be in the vacuum. However, due to the similar dielectric constants of the solute and the vacuum, it is reasonable to assume that such points can be treated as being in the solute phase.

It is important to note that different states can result in the same solute and solvent phases. For instance, consider the scenario where a solvent molecule and an ion are interchanged, which are originally located at different positions, within a given state. Allowing for a slight abuse of notation, we refer to the subset of states within \mathcal{S} that share the same solute and solvent phases as a *microstate* of the solute-solvent system. Assume that the system undergoes K microstates: $\mathcal{M}_1, \dots, \mathcal{M}_K \in \mathcal{F}$; and each \mathcal{M}_k occurs with a probability $p_k = \mathcal{P}(\mathcal{M}_k)$. For notational brevity, we put $\mathcal{K} = \{1, 2, \dots, K\}$. This leads to a decomposition $\mathcal{S} = \bigsqcup_{k \in \mathcal{K}} \mathcal{M}_k$;

and thus $\sum_{k \in \mathcal{K}} p_k = 1$.

We define several random variables that will be extensively used in this article.

- $X : \mathcal{S} \rightarrow \mathcal{K}$, where $X = \sum_{k \in \mathcal{K}} k \chi_{\mathcal{M}_k}$. Thus $X(\mathcal{S}_\alpha)$ indicates the microstate that \mathcal{S}_α belongs to.
- $\mathcal{C}_j : \mathcal{S} \rightarrow L^1(\Omega)$, where $\mathcal{C}_j(\mathcal{S}_\alpha) = \mathcal{C}_{\alpha,j}$ with $j \in \{0, 1, \dots, N_c\}$. Thus when $j \in \{1, \dots, N_c\}$, $\mathcal{C}_j(\mathcal{S}_\alpha)(x)$ is the (number) concentration of the j -th ion species at $x \in \Omega$ in \mathcal{S}_α ; $\mathcal{C}_0(\mathcal{S}_\alpha)(x)$ is the (number) concentration of the solvent molecule at $x \in \Omega$ in \mathcal{S}_α .

Let Z be a Banach space. The ensemble average of a random variable $Y : \mathcal{S} \rightarrow Z$ (in \mathcal{S}) is defined as

$$\langle Y \rangle := \mathbb{E}(Y) = \mathbb{E}[\mathbb{E}(Y|X = k)] = \sum_{k \in \mathcal{K}} p_k \mathbb{E}(Y|X = k). \quad (2.1)$$

Similarly, if one considers \mathcal{M}_k as a (statistic) ensemble, the ensemble average of Y in \mathcal{M}_k is defined by

$$\langle Y \rangle_k := \mathbb{E}(Y|X = k).$$

Throughout the remainder of this article, unless explicitly stated otherwise, the ensemble average of a quantity Y always refers to the object defined by (2.1).

2.2. A Sharp Interface VISM. In this section, we will introduce the solvation energy defined in a microstate \mathcal{M}_k with a fixed sharp solute-solvent interface. Assume that in microstate \mathcal{M}_k , the solute phase is represented by a Caccioppoli subset $D_k \subseteq \Omega$, or equivalently, $U_k = \Omega \setminus \bar{D}_k$ is the solvent phase. Then the solute-solvent interface is given by ∂D_k . See Figure 1(A) for an illustration.

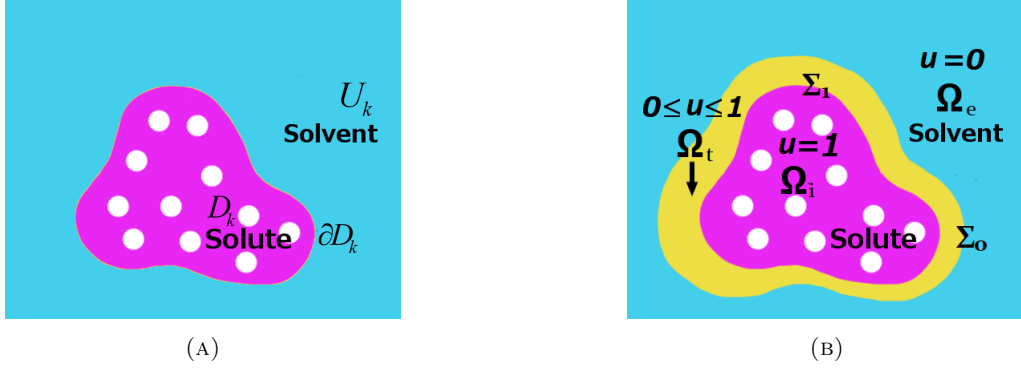


FIGURE 1. (A) Illustration of a microstate \mathcal{M}_k : D_k is the solute region; U_k is the solvent region; ∂D_k is the solute-solvent interface; (B) Domain decomposition for a grand canonical ensemble: Ω_i is the region occupied by the solute in all microstates; Ω_e denotes the region occupied by the solvent in all microstates; Ω_t denotes the transition region where $0 \leq u \leq 1$.

In this article, solute atoms are treated as hard spheres. More precisely, we consider the atom centered at x_i , $i = 1, \dots, N_m$, as a sphere of radius $\sigma_i > 0$, i.e., $B(x_i, \sigma_i)$, for which solvent molecules and ions cannot enter. On the other hand, the solvent and ion concentrations are the same as their bulk concentrations in regions sufficiently far away from the solute. As a consequence, such regions cannot be contained in the solute phase in any microstate. Based on these observations, we may assume that there are two open subsets, Ω_i and Ω_e , of Ω with $\bigcup_{i=1}^{N_m} \bar{B}(x_i, \sigma_i) \subset \Omega_i \subseteq \Omega \setminus \bar{\Omega}_e$ and $\partial\Omega \subset \partial\Omega_e$ such that

$$\Omega_i \subset D_k \subset \Omega \setminus \bar{\Omega}_e \quad \text{for all } k \in \mathcal{K}. \quad (2.2)$$

For instance, one can take Ω_i to be the region enclosed by a smoothed solvent excluded surface and Ω_e to be region outside a smoothed solvent accessible surface. Let $\Omega_t := \Omega \setminus (\bar{\Omega}_i \cup \bar{\Omega}_e)$ be the transition region. By Assumption (2.2), in all microstates,

- ions are located outside Ω_i , and
- the solute-solvent interfaces are located inside $\bar{\Omega}_t$.

In addition, we define $\Sigma_1 = \partial\Omega_i$ and $\Sigma_0 = \partial\Omega_e \setminus \partial\Omega$. We assume that Σ_0, Σ_1 are C^2 and Ω_t is connected so that $\Sigma_0 \cap \Sigma_1 = \emptyset$. See Figure 1(B) for an illustration.

The hydrophobicity of the amino acids in the biomolecule varies from position to position. To account for this phenomenon, we introduce a positive variable surface tension function $\theta \in C^1(\bar{\Omega}_t)$. Without loss of generality, we may extend θ to be a function in $C^1(\bar{\Omega})$, still denoted by θ , such that

$$\theta_0 \leq \theta(x) \leq \theta_1, \quad x \in \Omega$$

for some constants $0 < \theta_0 < \theta_1$. By [10, Lemma 1],

$$\int_{\Omega} \theta(x) d|Df(x)| = \sup \left\{ \int_{\Omega} f(x) \nabla \cdot (\theta(x) \phi(x)) dx : \phi \in C_c^1(\Omega; \mathbb{R}^3), \|\phi\|_{\infty} \leq 1 \right\}, \quad f \in BV(\Omega). \quad (2.3)$$

See [13] for the definition of BV -functions. It is clear that, for any $f \in BV(\Omega)$ with $f \equiv 0$ in Ω_e and $f \equiv 1$ in Ω_i , the value of $\int_{\Omega} \theta(x) d|Df(x)|$ is independent of how θ is extended outside $\bar{\Omega}_t$.

As proposed in [22, 23], the solvation free energy in microstate \mathcal{M}_k predicted by a sharp-interface VISM is the value of the following energy functional evaluated at χ_{D_k} :

$$\mathcal{E}(\chi_{D_k}) = I_{\text{np}}(\chi_{D_k}) + I_{\text{p}}(\chi_{D_k}, \psi),$$

where $\psi : \Omega \rightarrow \mathbb{R}$ is the electrostatic potential. The two components I_{np} and I_{p} are termed the nonpolar and polar portion of the solvation energy, respectively. For every fixed D_k , $\psi = \psi_{\chi_{D_k}}$ is chosen to maximize $I_{\text{p}}(\chi_{D_k}, \psi)$ among all ψ taking a predetermined Dirichlet boundary value ψ_D on $\partial\Omega$.

The nonpolar solvation energy consists of three parts:

$$I_{\text{np}}(\chi_{D_k}) = \int_{\Omega} \theta d|D\chi_{D_k}| + P_h \text{Vol}(D_k) + \int_{U_k} \rho_s U^{\text{vdW}}(x) dx.$$

When $\theta \equiv \gamma$ for some constant $\gamma > 0$, the first term reduces to $\gamma \text{Per}(D_k; \Omega)$ with $\text{Per}(D_k; \Omega)$ being the perimeter (in Ω) of the biomolecule region D_k . This term measures the disruption of intermolecular and/or intramolecular bonds that occurs when a surface is created. In addition, $\text{Vol}(D_k)$ represents the volume of D_k ; P_h is the (constant) hydrodynamic pressure. Therefore, $P_h \text{Vol}(D_k)$ is the mechanical work of creating the biomolecular size vacuum in the solvent. In the last integral, ρ_s is the (constant) solvent bulk density; and U^{vdW} represents the Lennard-Jones potential [48]; as such $U^{\text{vdW}} \in C^\infty(\overline{\Omega} \setminus \{x_1, \dots, x_{N_m}\})$.

Currently, one of the most widely-used polar solvation models is based on the Poisson-Boltzmann (PB) theory [1, 26, 27, 30, 35]. In the framework of classical PB theory, the polar energy is expressed as

$$I_{\text{p}}(\chi_{D_k}, \psi) = \int_{D_k} \left[\rho(x)\psi(x) - \frac{\epsilon_p}{8\pi} |\nabla\psi(x)|^2 \right] dx - \int_{U_k} \left[\frac{\epsilon_s}{8\pi} |\nabla\psi(x)|^2 + \beta^{-1} \sum_{j=1}^{N_c} c_j^\infty (e^{-\beta q_j \psi(x)} - 1) \right] dx, \quad (2.4)$$

where ρ is an L^∞ -approximation of the solute partial charges supported in $\bigcup_{i=1}^{N_m} B(x_i, \sigma_i)$. ϵ_p and ϵ_s are the dielectric constants of the solute and the solvent, respectively. Usually, $\epsilon_p \approx 1$ for the protein and $\epsilon_s \approx 80$ for the water. q_j is the charge of ion species j , $j = 1, 2, \dots, N_c$, and $\beta = 1/k_B T$, where k_B is the Boltzmann constant, T is the (constant) absolute temperature. c_j^∞ is the (constant) bulk concentration of the j -th ionic species. For notational brevity, we define

$$B(s) = \beta^{-1} \left[\sum_{j=1}^{N_c} c_j^\infty (e^{-\beta s q_j} - 1) \right], \quad s \in \mathbb{R}. \quad (2.5)$$

In addition, we assume the charge neutrality condition

$$\sum_{j=1}^{N_c} c_j^\infty q_j = 0. \quad (2.6)$$

It is important to observe that $B(0) = 0$ and, by (2.2), $B'(0) = 0$ and $B'(\pm\infty) = \pm\infty$. Further, $B''(s) > 0$. We thus conclude that $B(0) = \min_{s \in \mathbb{R}} B(s)$ and B is strictly convex.

To sum up, in microstate \mathcal{M}_k , the solvation energy is given by

$$\begin{aligned} \mathcal{E}(\chi_{D_k}) = & \int_{\Omega} \theta d|D\chi_{D_k}| + P_h \text{Vol}(D_k) + \int_{U_k} \rho_s U^{\text{vdW}}(x) dx + \int_{D_k} \left[\rho(x)\psi(x) - \frac{\epsilon_p}{8\pi} |\nabla\psi(x)|^2 \right] dx \\ & - \int_{U_k} \left[\frac{\epsilon_s}{8\pi} |\nabla\psi(x)|^2 + B(\psi(x)) \right] dx, \end{aligned} \quad (2.7)$$

where $\psi = \psi_{\chi_{D_k}}$ solves the PB equation:

$$\nabla \cdot ((\epsilon_p \chi_{D_k} + \epsilon_s \chi_{U_k}) \nabla \psi) - 4\pi \chi_{U_k} B'(\psi) + 4\pi \rho = 0 \quad \text{in } \Omega \quad (2.8)$$

in the admissible set

$$\mathcal{A} = \{\psi \in H^1(\Omega) : \psi|_{\partial\Omega} = \psi_D\} \quad \text{for some } \psi_D \in W^{1,\infty}(\Omega). \quad (2.9)$$

Remark 2.1. Now, we will present a concise discussion regarding the expression for polar energy expression (2.2). This discussion will serve as a crucial foundation for the derivation of EASE. To begin, let us review the definitions of the random variables X and \mathcal{C}_j defined in Section 2.1.

A pivotal element of the Poisson-Boltzmann theory is an electrostatic potential ψ , which is identical across all states within a fixed (statistical) ensemble under consideration. Consider a fixed microstate \mathcal{M}_k as a (statistical) ensemble. In \mathcal{M}_k , the electrostatic potential ψ satisfies the fundamental equation of electrostatics,

the Poisson equation:

$$-\nabla \cdot [(\epsilon \chi_{D_k} + \epsilon_s \chi_{U_k}) \nabla \psi] = 4\pi \left(\rho + \sum_{j=1}^{N_c} q_j c_j^k \right), \quad (2.10)$$

where c_j^k is the (number) concentration of the j -th ion speices in \mathcal{M}_k , i.e.

$$c_j^k = \langle \mathcal{C}_j \rangle_k = \mathbb{E}(\mathcal{C}_j | X = k); \quad (2.11)$$

and thus $c_j^k \equiv 0$ in D_k . However, since the probability distribution of \mathcal{C}_j is unknown, it is impossible to directly compute c_j^k by means of (2.1). Indeed, the expression of c_j^k should be derived from the Helmholtz free energy, cf. [26, 31, 37].

To find the Helmholtz free energy H_k in \mathcal{M}_k , we consider the random variable $E_\psi : \mathcal{S} \rightarrow \mathbb{R}$, where

$$E_\psi(\mathcal{S}_\alpha) = \int_{D_k} \left(\rho \psi - \frac{\epsilon_p}{8\pi} |\nabla \psi|^2 \right) dx + \int_{U_k} \left[\sum_{j=1}^{N_c} (q_j \mathcal{C}_{\alpha,j} \psi - \mathcal{C}_{\alpha,j} \mu_j^\infty) - \frac{\epsilon_s}{8\pi} |\nabla \psi|^2 \right] dx \quad (2.12)$$

is the internal energy in state \mathcal{S}_α with μ_j^∞ being the chemical potential of the j -th ion species, which is uniform everywhere in a grand canonical ensemble. Then the ensemble average of E_ψ in \mathcal{M}_k is given by

$$\langle E_\psi \rangle_k = \mathbb{E}(E_\psi | X = k) = \int_{D_k} \left(\rho \psi - \frac{\epsilon_p}{8\pi} |\nabla \psi|^2 \right) dx + \int_{U_k} \left[\sum_{j=1}^{N_c} (q_j c_j^k \psi - c_j^k \mu_j^\infty) - \frac{\epsilon_s}{8\pi} |\nabla \psi|^2 \right] dx. \quad (2.13)$$

Meanwhile, within the framework of classic PB theory, the entropy S_k in \mathcal{M}_k is given by

$$-TS_k = \beta^{-1} \int_{U_k} \sum_{j=1}^{N_c} c_j^k [\ln(\mathbf{v} c_j^k) - 1] dx, \quad (2.14)$$

where $1/\mathbf{v}$ is a reference concentration. It is crucial to highlight that, in statistic mechanics, entropy is not a random variable of $(\mathcal{S}, \mathcal{F}, \mathcal{P})$ and should not be obtained by ensemble averaging its counterparts in all states. The Helmholtz free energy H_k is given by $H_k = \langle E_\psi \rangle_k - TS_k$. Equating the first variation of H_k with respect to c_j^k to zero gives

$$\mu_j^\infty = \beta^{-1} \ln(\mathbf{v} c_j^k(x)) + q_j \psi(x) \quad \text{in } U_k.$$

This leads to the relation $c_j^k(x) = \chi_{U_k}(x) \mathbf{v}^{-1} e^{\beta \mu_j^\infty} e^{-\beta q_j \psi(x)}$. When x is sufficient far away from the solute, we have $\psi(x) = 0$ and $c_j^k(x) = c_j^\infty$. This implies that $c_j^\infty = \mathbf{v}^{-1} e^{\beta \mu_j^\infty}$. Hence we obtain the relation

$$c_j^k(x) = \chi_{U_k}(x) c_j^\infty e^{-\beta q_j \psi(x)}. \quad (2.15)$$

This is exactly the Boltzmann distribution. It is important to emphasize that the term χ_{U_k} in Equation (2.1) arises from the fact that, in H_k , the domain of integration for any integral involving c_j^k is restricted to U_k . This restriction is necessary because $c_j^k \equiv 0$ within the domain D_k . By using the characteristic function χ_{U_k} , we ensure that the integration is performed only over the relevant region U_k where c_j^k is nonzero. Plugging (2.1) back into the expression of H_k yields

$$H_k = \int_{D_k} \left(\rho(x) \psi(x) - \frac{\epsilon_p}{8\pi} |\nabla \psi(x)|^2 \right) dx - \int_{U_k} \left(\frac{\epsilon_s}{8\pi} |\nabla \psi(x)|^2 + \beta^{-1} \sum_{j=1}^{N_c} c_j^\infty e^{-\beta q_j \psi(x)} \right) dx. \quad (2.16)$$

Since the polar energy equals zero when ψ vanishes everywhere, following [44], a constant term

$$\beta^{-1} \int_{U_k} \sum_{j=1}^{N_c} c_j^\infty dx \quad (2.17)$$

should be added to (2.1), which yields the polar energy expression (2.2) in \mathcal{M}_k . Note that $\sum_{j=1}^{N_c} q_j c_j^k = -\chi_{U_k} B'(\psi)$, see (2.2). Plugging this expression into (2.1) shows that ψ solves (2.2). By Lemma A.1, ψ maximizes $I_p(\chi_{D_k}, \cdot)$ in \mathcal{A} .

To summarize, within the framework of the classic Poisson-Boltzmann theory, the following points are crucial in the derivation of EASE in a fixed ensemble:

- **Universal Electrostatic Potential:** It is necessary to use a universal electrostatic potential, denoted as ψ , which applies across all microstates, when deriving the Boltzmann distribution. This potential is independent of specific microstates and is used consistently in the calculations.
- **Non-Random Nature of Entropy:** In the context of EASE, it is important to note that one component of the solvation energy, namely entropy, is not considered a random variable of the system $(\mathcal{S}, \mathcal{F}, \mathcal{P})$. Therefore, when calculating the entropy within EASE, it should not be obtained by averaging its counterpart in the individual microstates.

By considering these factors, EASE can be derived within a fixed ensemble, incorporating an appropriate electrostatic potential and accounting for the non-random nature of entropy.

3. MODELING OF ENSEMBLE AVERAGE SOLVATION ENERGY

If one tries to directly use (2.1) and compute EASE, an obvious barrier is how to calculate the probability p_k . Although, according to statistical mechanics, p_k can be obtained by means of the Boltzmann weight, an accurate approximation of the Boltzmann weight requires a sufficiently large sampling of microstates, which creates a significant computational burden. Indeed, in the routine calculation of the EASE, one needs to carry out certain explicit solvent simulations, e.g. molecular dynamics (MD), to obtain thousands of solute-solvent states and perform energy calculations for each state.

The core of our modeling paradigm is, instead of ensemble averaging the outputs of the solvation energy functional (2.2), one should ensemble average the inputs, i.e. χ_{D_k} , to obtain a diffuse-interface profile. Then the EASE can be computed by using this one profile instead of thousand of solute-solvent states. This leads to the following definition:

$$u = \sum_{k \in \mathcal{K}} p_k \chi_{D_k}.$$

As such, $u(x)$ represents the probability of $x \in \Omega$ found in the solute phase among all microstates. Figure 1(B) shows the range of u in different regions. The definition of u enforces the following physical constraints

$$u(x) \in [0, 1] \quad \text{for a.a. } x \in \Omega \quad (3.1)$$

and

$$u = 1 \quad \text{a.e. in } \Omega_i \quad \text{and} \quad u = 0 \quad \text{a.e. in } \Omega_e. \quad (3.2)$$

Then the admissible set for u is defined as

$$\mathcal{X} = \{u \in BV(\Omega) : u \text{ satisfies Constraints (3) and (3)}\}.$$

To construct the EASE functional, we introduce the following functions defined on \mathcal{K} :

$$\begin{aligned} f_D : \mathcal{K} &\rightarrow BV(\Omega), \quad f_D(k) = \chi_{D_k} \\ f_U : \mathcal{K} &\rightarrow BV(\Omega), \quad f_U(k) = \chi_{U_k} \\ f_s : \mathcal{K} &\rightarrow \mathbb{R}, \quad f_s(k) = \int_{\Omega} \theta d|D\chi_{D_k}| \\ f_i : \mathcal{K} &\rightarrow \mathcal{L}(L^1(\Omega), \mathbb{R}) = L^\infty(\Omega), \quad f_i(k)v = \int_{\Omega} \chi_{D_k} v dx = \int_{D_k} v dx, \quad v \in L^1(\Omega) \\ f_e : \mathcal{K} &\rightarrow \mathcal{L}(L^1(\Omega), \mathbb{R}) = L^\infty(\Omega), \quad f_e(k)v = \int_{\Omega} \chi_{U_k} v dx = \int_{U_k} v dx, \quad v \in L^1(\Omega). \end{aligned}$$

The ensemble averages of all bulk and interfacial energy components can be derived from the above functions. For example,

- the ensemble average of interfacial energy, i.e. $\int_{\Omega} \theta d|D\chi_{D_k}|$, is given by $\langle f_s(X) \rangle$;
- the ensemble average of the term $P_h \text{Vol}(D_k)$ is given by $\langle f_i(X) P_h \rangle$;
- the ensemble average of the term $\int_{U_k} \rho_s U^{\text{vdW}} dx$, is given by $\langle f_e(X) (\rho_s U^{\text{vdW}}) \rangle$.

Proposition 3.1. *Assume that $v \in L^1(\Omega)$ is an energy density function. Then the ensemble average of the energy stored in the solute and solvent phases can be computed as follows:*

$$\langle f_i(X)v \rangle = \int_{\Omega} uv \, dx \quad \text{and} \quad \langle f_e(X)v \rangle = \int_{\Omega} (1-u)v \, dx.$$

Proof. The proof is straightforward. Indeed, we will only check the equality for $\langle f_i(X)v \rangle$. Consider the random variable $f_i(X)v : \mathcal{S} \rightarrow \mathbb{R}$. Then

$$\langle f_i(X)v \rangle = \mathbb{E}[\mathbb{E}(f_i(X)v|X=k)] = \sum_{k \in \mathcal{K}} p_k \int_{D_k} v \, dx = \int_{\Omega} \sum_{k \in \mathcal{K}} p_k \chi_{D_k} v \, dx = \int_{\Omega} uv \, dx.$$

□

Following the discussion in Remark 2.1, let $\psi : \Omega \rightarrow \mathbb{R}$ be the universal electrostatic potential ψ , which is identical among all \mathcal{S}_{α} . To formulate the Poisson equation, we notice that the dielectric function $\epsilon_p f_D(k) + \epsilon_s f_U(k) = \epsilon_p \chi_{D_k} + \epsilon_s \chi_{U_k}$ in (2.1) should be replaced by the ensemble averaged one:

$$\epsilon(u) := \mathbb{E}(\epsilon_p f_D(X) + \epsilon_s f_U(X)) = u\epsilon_p + (1-u)\epsilon_s.$$

Hence $\psi \in \mathcal{A}$ solves

$$-\nabla \cdot [\epsilon(u)\nabla\psi] = 4\pi \left(\rho + \sum_{j=1}^{N_c} q_j c_j \right) \quad \text{in } \Omega, \quad (3.3)$$

where c_j is the ion concentration of the j -th ion species in the ensemble under consideration, i.e.

$$c_j = \mathbb{E}(C_j) = \mathbb{E}[\mathbb{E}(C_j|X=k)] = \sum_{k \in \mathcal{K}} p_k c_j^k = \sum_{k \in \mathcal{K}} p_k c_j^k \chi_{U_k}. \quad (3.4)$$

Note that the function $c_j \equiv 0$ in the set $\{u = 1\} := \{x \in \Omega : u(x) = 1\}$. By a similar argument to Remark 2.1 and Proposition 3.1, the ensemble average of E_{ψ} , cf. (2.1) and (2.1), equals

$$\begin{aligned} \langle E_{\psi} \rangle &= \sum_{k \in \mathcal{K}} p_k \left[\int_{D_k} \left(\rho\psi - \frac{\epsilon_p}{8\pi} |\nabla\psi|^2 \right) dx + \int_{U_k} \left(\sum_{j=1}^{N_c} (q_j c_j^k \psi - c_j^k \mu_j^{\infty}) - \frac{\epsilon_s}{8\pi} |\nabla\psi|^2 \right) dx \right] \\ &= \int_{\Omega} \left[\rho\psi + \sum_{j=1}^{N_c} (q_j c_j \psi - c_j \mu_j^{\infty}) - \frac{\epsilon(u)}{8\pi} |\nabla\psi|^2 \right] dx. \end{aligned} \quad (3.5)$$

In the following two subsections, we will derive two functionals for the EASE within the frameworks of classic PB theory and size-modified PB theory.

3.1. Classic Poisson-Boltzmann Theory. In this subsection, we will first consider the classic PB theory, in which ions and solvent molecules are assumed to be point-like and have no correlation between their concentrations.

3.1.1. Ensemble Average Polar Energy. In the classic PB theory framework, the entropy can be formulated as

$$-TS = \beta^{-1} \int_{\{u < 1\}} \sum_{j=1}^{N_c} c_j [\ln(vc_j) - 1] \, dx.$$

The domain of integration $\{u < 1\} = \{x \in \Omega : u(x) < 1\}$ is due to the fact that c_j vanishes identically in $\{u = 1\}$. Applying a similar argument leading to (2.1) to the Helmholtz energy $H = \langle E_{\psi} \rangle - ST$, one can obtain the Boltzmann distribution

$$c_j = \chi_{\{u < 1\}} c_j^{\infty} e^{-\beta q_j \psi}. \quad (3.6)$$

After plugging (3.1.1) into H , as in (2.1), the constant term

$$\beta^{-1} \int_{\Omega} \chi_{\{u < 1\}} \sum_{j=1}^{N_c} c_j^{\infty} \, dx \quad (3.7)$$

needs to be added to H to adjust the reference state of the zero energy in the ensemble under consideration. Finally, we arrive at the ensemble average polar energy

$$I_p(u, \psi) = H + \beta^{-1} \int_{\Omega} \chi_{\{u < 1\}} \sum_{j=1}^{N_c} c_j^{\infty} dx = \int_{\Omega} \left[\rho \psi - \frac{\epsilon(u)}{8\pi} |\nabla \psi|^2 - \chi_{\{u < 1\}} B(\psi) \right] dx.$$

On the other hand, replacing c_j in (3) by (3.1.1) shows that $\psi \in \mathcal{A}$ solves the generalized PB equation:

$$\nabla \cdot [\epsilon(u) \nabla \psi] - 4\pi \chi_{\{u < 1\}} B'(\psi) + 4\pi \rho = 0 \quad \text{in } \Omega. \quad (3.8)$$

Lemma A.1 shows that ψ maximizes $I_p(u, \cdot)$ in \mathcal{A} for any fixed $u \in \mathcal{X}$.

3.1.2. Ensemble Average Interfacial Energies. Following the discussions in Section 3.1.1, the EASE in the framework of classic PB theory can be represented by

$$\langle f_s(X) \rangle + L(u), \quad \text{where } L(u) = \int_{\Omega} [P_h u + \rho_s(1-u)U^{\text{vdW}}] dx + I_p(u, \psi_u)$$

with ψ_u maximizing $I_p(u, \cdot)$ in \mathcal{A} . It only remains to compute the ensemble averaged interfacial energy

$$\langle f_s(X) \rangle = \mathbb{E}[\mathbb{E}(f_s(X) | X = k)] = \sum_{k \in \mathcal{K}} p_k \int_{\Omega} \theta d|D\chi_{D_k}|.$$

Proposition 3.3 below shows that the integral $\int_{\Omega} \theta d|Du|$ can be used to approximate the ensemble averaged interfacial energy. Before proving Proposition 3.3, we will need the following lemma.

Lemma 3.2. *Let $\{D_k\}_{k \in \mathcal{K}}$ be a family of Caccioppoli sets satisfying $\Omega_i \subset D_k \subset \Omega \setminus \overline{\Omega}_e$ and $p_k \in [0, 1]$ with $\sum_{k \in \mathcal{K}} p_k = 1$. Then for each $\varepsilon > 0$, there exists another family $\{\tilde{D}_k\}_{k \in \mathcal{K}}$ of Caccioppoli sets satisfying $\Omega_i \subset \tilde{D}_k \subset \Omega \setminus \overline{\Omega}_e$ and*

$$\mathcal{H}^2(\partial^* \tilde{D}_k \cap \partial^* \tilde{D}_j) = 0, \quad \forall k, j \in \mathcal{K}, \quad k \neq j, \quad (3.9)$$

with $\partial^* D$ being the reduced boundary of a Caccioppoli set D . Moreover,

$$\left| \sum_{k \in \mathcal{K}} p_k \int_{\Omega} \theta d|D\chi_{D_k}| + L(u) - \sum_{k \in \mathcal{K}} p_k \int_{\Omega} \theta d|D\chi_{\tilde{D}_k}| - L(\tilde{u}) \right| < \varepsilon,$$

where $u = \sum_{k \in \mathcal{K}} p_k \chi_{D_k}$ and $\tilde{u} = \sum_{k \in \mathcal{K}} p_k \chi_{\tilde{D}_k}$.

Proof. In view of Lemma A.2, it suffices to construct a family of Caccioppoli sets $\{D_{k,n}\}_{n=1}^{\infty}$ satisfying Assumption (3.2) and $\Omega_i \subset D_{k,n} \subset \Omega \setminus \overline{\Omega}_e$ such that

$$\lim_{n \rightarrow \infty} \|\chi_{D_k} - \chi_{D_{k,n}}\|_{L^1} = 0, \quad \lim_{n \rightarrow \infty} \int_{\Omega} \theta d|D\chi_{D_{k,n}}| = \int_{\Omega} \theta d|D\chi_{D_k}|. \quad (3.10)$$

Indeed, letting $u_n = \sum_{k \in \mathcal{K}} p_k \chi_{D_{k,n}}$, (3.1.2) implies that $u_n \rightarrow u$ and $\chi_{\{u_n < 1\}} \rightarrow \chi_{\{u < 1\}}$ in $L^1(\Omega)$. Then it follows from Lemma A.2 and the dominated convergence theorem that $L(u_n, \psi_{u_n}) \rightarrow L(u, \psi_u)$ as $n \rightarrow \infty$.

Because Σ_i , $i = 0, 1$, are C^2 , there exists some $a > 0$ such that Σ_i has a tubular neighborhood $B_a(\Sigma_i)$ of width $a > 0$, cf. [28, Exercise 2.11] and [36, Remark 3.1]. For sufficiently small $r \in (0, a)$, let

$$D_k^r = (D_k \cup B_r(\Sigma_1)) \setminus B_r(\Sigma_0).$$

In view of the relation $\text{Per}(S \cup T; \Omega) + \text{Per}(S \cap T; \Omega) \leq \text{Per}(S; \Omega) + \text{Per}(T; \Omega)$ for any Caccioppoli sets $S, T \subset \Omega$, D_k^r are again Caccioppoli sets. Recall that $\text{Per}(S; \Omega)$ is the perimeter of S in Ω . According to Lemma 4.6, we have

$$\lim_{r \rightarrow 0^+} \|\chi_{D_k} - \chi_{D_k^r}\|_{L^1} = 0, \quad \lim_{r \rightarrow 0^+} \int_{\Omega} \theta d|\chi_{D_k^r}| = \int_{\Omega} \theta d|\chi_{D_k}|.$$

Note that the proof of Lemma 4.6 is independent of other results in this article. Therefore, without loss of generality, we may assume that for some sufficiently small $r > 0$

$$\Omega_i \cup B(\Sigma_1, r) \subset D_k \subset \Omega \setminus (\overline{\Omega}_e \cup B_r(\Sigma_0)).$$

Claim 1: For every k , there exists a sequence $\{f_{k,j}\}_{j=1}^\infty \subset C^\infty(\bar{\Omega})$ such that $0 \leq f_{k,j} \leq 1$ a.e. in Ω and

$$\lim_{j \rightarrow \infty} \|\chi_{D_k} - f_{k,j}\|_{L^1} = 0, \quad \lim_{j \rightarrow \infty} \int_{\Omega} \theta d|Df_{k,j}| = \int_{\Omega} \theta d|\chi_{D_k}|.$$

Proof of Claim 1. We consider χ_{D_k} as an element in $BV(\mathbb{R}^3)$. Choose a sequence $\varepsilon_j \rightarrow 0^+$ and define $f_{k,j} := \eta_{\varepsilon_j} * \chi_{D_k}$, where η_{ε_j} is the standard Friedrichs mollifying kernel. Then $\lim_{j \rightarrow \infty} \|\chi_{D_k} - f_{k,j}\|_{L^1} = 0$.

[10, Corollary 1] implies that $\int_{\Omega} \theta d|\chi_{D_k}(x)| \leq \liminf_{j \rightarrow \infty} \int_{\Omega} \theta d|f_{k,j}(x)|$. Note that $f_{k,j} \in \mathcal{X} \cap C^\infty(\bar{\Omega})$ for sufficiently large j . For any $\phi \in C_0^1(\Omega; \mathbb{R}^3)$ with $\|\phi\|_\infty \leq 1$, it follows from [10, Lemma 1] that

$$\begin{aligned} \int_{\Omega} f_{k,j} \nabla \cdot (\theta \phi) dx &= \int_{\Omega} (\eta_{\varepsilon_j} * \chi_{D_k}) \nabla \cdot (\theta \phi) dx = \int_{\Omega} \chi_{D_k} \nabla \cdot [\eta_{\varepsilon_j} * (\theta \phi)] dx \\ &= \int_{\Omega} \chi_{D_k} \nabla \cdot \left[\theta \left(\frac{\eta_{\varepsilon_j} * (\theta \phi)}{\theta} \right) \right] dx \\ &\leq \|(\eta_{\varepsilon_j} * \theta)/\theta\|_{L^\infty} \int_{\Omega} \theta d|\chi_{D_k}(x)|. \end{aligned}$$

Here $(\eta_{\varepsilon_j} * \theta)(x) = \int_{\Omega} \eta_{\varepsilon_j}(x-y) \theta(y) dy$ for $x \in \Omega$. Taking supremum over all such ϕ , we derive that

$$\int_{\Omega} \theta d|f_{k,j}(x)| \leq \|(\eta_{\varepsilon_j} * \theta)/\theta\|_{L^\infty} \int_{\Omega} \theta d|\chi_{D_k}(x)|.$$

By the uniform continuity of θ , it is not a hard task to verify that $\lim_{j \rightarrow \infty} \|(\eta_{\varepsilon_j} * \theta)/\theta\|_{L^\infty(\Omega)} = 1$. Therefore, the above inequality implies that $\limsup_{j \rightarrow \infty} \int_{\Omega} \theta d|f_{k,j}(x)| \leq \int_{\Omega} \theta d|\chi_{D_k}(x)|$. \blacksquare

By the Sard's Theorem, there exists some $S \subset (0, 1)$ with $\mathcal{L}^1((0, 1) \setminus S) = 0$ such that, for all $t \in S$, the super-level set $E_{k,j}^t = \{f_{k,j} > t\}$ has a smooth boundary. The coarea formula implies that

$$\int_{\Omega} \theta d|\chi_{D_k}| = \lim_{j \rightarrow \infty} \int_{\Omega} \theta d|f_{k,j}| = \lim_{j \rightarrow \infty} \int_0^1 \int_{\Omega} \theta d|\chi_{E_{k,j}^t}| dt \geq \int_0^1 \liminf_{j \rightarrow \infty} \int_{\Omega} \theta d|\chi_{E_{k,j}^t}| dt.$$

Therefore, for some $t \in S$,

$$\liminf_{j \rightarrow \infty} \int_{\Omega} \theta d|\chi_{E_{k,j}^t}| \leq \int_{\Omega} \theta d|\chi_{D_k}|.$$

Pick the subsequence $\{j_n\}_{n=1}^\infty$ such that

$$\liminf_{j \rightarrow \infty} \int_{\Omega} \theta d|\chi_{E_{k,j}^t}| = \lim_{n \rightarrow \infty} \int_{\Omega} \theta d|\chi_{E_{k,j_n}^t}|.$$

On the other hand, we can infer from the Chebyshev's Theorem that

$$\mathcal{L}^3(E_{k,j_n}^t \setminus D_k) \leq \frac{1}{t} \|f_{k,j_n} - \chi_{D_k}\|_{L^1}, \quad \mathcal{L}^3(D_k \setminus E_{k,j_n}^t) \leq \frac{1}{1-t} \|f_{k,j_n} - \chi_{D_k}\|_{L^1}.$$

This implies that

$$\lim_{n \rightarrow \infty} \|\chi_{E_{k,j_n}^t} - \chi_{D_k}\|_{L^1} = 0.$$

Therefore, it follows from [10, Corollary 1] that $\tilde{D}_{k,n} = E_{k,j_n}^t$ satisfies (3.1.2) with $D_{k,n}$ replaced by $\tilde{D}_{k,n}$.

Assume that $\mathcal{H}^2(\partial \chi_{\tilde{D}_{k,n}} \cap \partial \chi_{\tilde{D}_{j,n}}) > 0$ for some $k, j \in \mathcal{K}$ and $k \neq j$. Since $\partial \tilde{D}_{k,n}$ is C^2 , there exists some $a > 0$ such that $\partial \tilde{D}_{k,n}$ has a tubular neighborhood $B_a(\partial \tilde{D}_{k,n})$ of width $a > 0$. Denote by ν the outward unit normal of $\tilde{D}_{k,n}$ pointing into $\Omega \setminus \tilde{D}_{k,n}$. Then the map defined by

$$\Lambda : \partial \tilde{D}_{k,n} \times (-a, a) \rightarrow B_a(\partial \tilde{D}_{k,n}) : (x, r) \mapsto x + r\nu(x),$$

is a C^1 -diffeomorphism. Let $\Gamma_r := \Lambda(\partial \tilde{D}_{k,n}, r)$. Then, for every $i \in \mathcal{K}$, there are at most countably many $r \in (-a, a)$ such that $\mathcal{H}^2(\Gamma_r \cap \partial \chi_{\tilde{D}_{i,n}}) > 0$. Hence we can find $r \in (-a, a)$ sufficiently close to 0 such that

$$\mathcal{H}^2(\Gamma_r \cap \partial \chi_{\tilde{D}_{i,n}}) = 0, \quad \forall i \in \mathcal{K}$$

and $\Gamma_r \subset \Omega_t$ and

$$\left\| \chi_{D_{k,n}} - \chi_{\tilde{D}_{k,n}} \right\|_{L^1} + \left| \int_{\Omega} \theta d|D\chi_{D_{k,n}}| - \int_{\Omega} \theta d|D\chi_{\tilde{D}_{k,n}}| \right| < 1/n,$$

where $D_{k,n}$ is the region enclosed by Γ_r . Modifying all $\tilde{D}_{k,n}$, $k \in \mathcal{K}$, in such a way yields a family of smooth sets $\{D_{k,n}\}_{k \in \mathcal{K}}$ satisfying $\Omega_i \subset D_{k,n} \subset \Omega \setminus \bar{\Omega}_e$ and Assumptions (3.2) and (3.1.2). \square

The lemma above elucidates that within a given ensemble, slight adjustments can be made to the solute regions $\{D_k\}_{k \in \mathcal{K}}$ in order to attain (3.2), while ensuring that the alterations in the associated solvation energy remain “infinitesimally” negligible. Consequently, it is permissible to consistently presume that $\{D_k\}_{k \in \mathcal{K}}$ adheres to (3.2).

Proposition 3.3. *Assume that $\{D_k\}_{k \in \mathcal{K}}$ satisfies (3.2). Then*

$$\int_{\Omega} \theta d|Du| = \sum_{k \in \mathcal{K}} p_k \int_{\Omega} \theta d|D\chi_{D_k}|.$$

Proof. By the De Giorgi’s structure theorem, cf. [24, Theorem 5.7.2], χ_{D_k} are 2-rectifiable, i.e. there exist Borel sets F_k and C^1 -functions $g_{k,n} : U_{k,n} \rightarrow \mathbb{R}^3$, $U_{k,n} \subset \mathbb{R}^2$ compact, such that $\|\partial D_k\|(F_k) = 0$ and

$$\partial^* D_k = F_k \cup \bigcup_{n=1}^{\infty} g_{k,n}(U_{k,n}).$$

Pick arbitrary $\varepsilon > 0$. For every $k \in \mathcal{K}$, we can find $N_k = N_k(\varepsilon)$ such that

$$\|\partial D_k\|(\Omega \cap \bigcup_{n=N_k+1}^{\infty} g_{k,n}(U_{k,n})) \leq \frac{\varepsilon}{K\theta_1 p_k}.$$

Recall $K = |\mathcal{K}|$. Therefore, we obtain compact sets

$$G_{k,\varepsilon} := \bigcup_{n=1}^{N_k(\varepsilon)} g_{k,n}(U_{k,n}), \quad k \in \mathcal{K}, \quad \text{and} \quad G_{\varepsilon} := \bigcup_{k \in \mathcal{K}} G_{k,\varepsilon}.$$

By the definition of the reduced boundary, the unit normal ν exists everywhere on G_{ε} . By the Urysohn’s Lemma, there exists a continuous function $\phi : \mathbb{R}^3 \rightarrow \mathbb{R}^3$ such that $\phi|_{G_{\varepsilon}} = \nu$. Restricting ϕ on $\bar{\Omega}$ and applying Stone-Weierstrass, we can find a smooth function $\phi_{\varepsilon} : \bar{\Omega} \rightarrow \mathbb{R}^3$ such that

$$\|\phi_{\varepsilon} - \phi\|_{L^{\infty}(G_{\varepsilon})} < \varepsilon.$$

Then, in a neighborhood $H \Subset \Omega$ of G_{ε} , we have $|\phi_{\varepsilon}| > 1/2$. Pick $h \in C_0^{\infty}(\Omega; [0, 1])$ such that $h \equiv 1$ in H . Setting $\psi_{\varepsilon}(x) = h(x) \frac{\phi_{\varepsilon}(x)}{|\phi_{\varepsilon}(x)|}$, it is an easy task to check that

$$1 \geq \psi_{\varepsilon}(x) \cdot \nu(x) \geq \frac{1 - \varepsilon}{1 + \varepsilon}, \quad x \in G_{\varepsilon}.$$

By [10, Lemma 1], we can estimate

$$\begin{aligned} \int_{\Omega} \theta d|Du| &\geq \int_{\Omega} (\theta \psi_{\varepsilon}) \cdot dDu = \sum_{k \in \mathcal{K}} p_k \int_{\Omega} \theta \psi_{\varepsilon} \cdot D\chi_{D_k} dx \geq \sum_{k \in \mathcal{K}} p_k \int_{G_{k,\varepsilon}} \theta \psi_{\varepsilon} \cdot D\chi_{D_k} dx - \varepsilon \\ &\geq \sum_{k \in \mathcal{K}} \frac{p_k(1 - \varepsilon)}{1 + \varepsilon} \int_{G_{k,\varepsilon}} \theta d|D\chi_{D_k}| - \varepsilon \\ &= \sum_{k \in \mathcal{K}} \frac{p_k(1 - \varepsilon)}{1 + \varepsilon} \left(\int_{\Omega} \theta d|D\chi_{D_k}| - \int_{\Omega \setminus G_{k,\varepsilon}} \theta d|D\chi_{D_k}| \right) - \varepsilon \\ &\geq \sum_{k \in \mathcal{K}} \frac{p_k(1 - \varepsilon)}{1 + \varepsilon} \int_{\Omega} \theta d|D\chi_{D_k}| - \frac{2\varepsilon}{1 + \varepsilon}. \end{aligned}$$

Since ε is arbitrary, we have

$$\int_{\Omega} \theta d|Du| \geq \sum_{k \in \mathcal{K}} p_k \int_{\Omega} \theta d|D\chi_{D_k}|.$$

The inverse inequality is obvious. We have thus proved the assertion. \square

3.1.3. *Total Energy Functional.* Based on Propositions 3.1 and 3.3, the ensemble average nonpolar energy can be formulated as

$$I_{\text{np}}(u) = \int_{\Omega} \theta d|Du| + \int_{\Omega} [P_h u + \rho_s(1-u)U^{\text{vdW}}] dx.$$

Therefore, the EASE functional is given by

$$\mathcal{E}(u) = \int_{\Omega} \theta d|Du| + \int_{\Omega} [P_h u + \rho_s(1-u)U^{\text{vdW}}] dx + \int_{\Omega} \left[\rho\psi - \frac{\epsilon(u)}{8\pi} |\nabla\psi|^2 - \chi_{\{u<1\}} B(\psi) \right] dx \quad (3.11)$$

with admissible set \mathcal{X} and $\psi = \psi_u \in \mathcal{A}$ is determined via the generalized PB equation (3.1.1).

3.2. Size-modified Poisson-Boltzmann Theory. In the classic PB theory, ionic solvents are assumed to be ideal: all ions and solvent molecules are point-like and there is no correlation between the (number) concentrations of these particles. However, the ideal ionic solvent assumption overlooks the crucial finite size effect of mobile ions and solvent molecules. Numerical simulations have demonstrated that the point-like ion assumption in classic PB theory can lead to nonphysically large ion concentrations near charged surfaces [7].

We will follow the idea in the pioneering work [5] by Bikerman to derive the size-modified polar energy formulation. Assume that each mobile ion and solvent molecule occupies a finite volume v . Building upon the definition of \mathcal{C}_0 introduced in Section 2.1, we define

$$c_0^k = \mathbb{E}(\mathcal{C}_0 | X = k) \quad \text{and} \quad c_0 = \mathbb{E}(\mathcal{C}_0) = \sum_{k \in \mathcal{K}} p_k c_0^k.$$

It is assumed that inside the solvent phase, apart from the occupancy of ions, the remaining space is filled with solvent molecules. In this context, the following relation holds:

$$v \sum_{j=0}^{N_c} c_j^k(x) = \chi_{U_k}(x), \quad x \in \Omega. \quad (3.12)$$

This relation enforces a maximum concentration of v^{-1} for each ion species. (3.2) implies that

$$c_0 = \sum_{k \in \mathcal{K}} p_k c_0^k = \sum_{k \in \mathcal{K}} p_k \left(v^{-1} - \sum_{j=1}^{N_c} c_j^k \right) \chi_{U_k} = v^{-1}(1-u) - \sum_{j=1}^{N_c} c_j, \quad (3.13)$$

Following [5], we can include the solvent entropic contribution and then the size-modified entropy S_{md} can be written as

$$\begin{aligned} -TS_{md} &= \beta^{-1} \int_{\{u<1\}} \sum_{j=0}^{N_c} c_j [\ln(vc_j) - 1] dx \\ &= \beta^{-1} \int_{\{u<1\}} \sum_{j=1}^{N_c} c_j [\ln(vc_j) - 1] dx \\ &\quad + \beta^{-1} \int_{\{u<1\}} \left(v^{-1}(1-u) - \sum_{j=1}^{N_c} c_j \right) \left[\ln \left((1-u) - v \sum_{j=1}^{N_c} c_j \right) - 1 \right] dx. \end{aligned}$$

See also [6, 7, 32, 33] for some related work.

Following the discussion in Remark 2.1, the variation of $H_{md} = \langle E_{\psi} \rangle - TS_{md}$, cf. (3), with respect to c_j , $j = 1, \dots, N_c$, gives

$$\mu_j^{\infty} = q_j \psi + \beta^{-1} \left[\ln(vc_j) - \ln \left((1-u) - v \sum_{i=1}^{N_c} c_i \right) \right] \chi_{\{u<1\}}.$$

This leads to the relation

$$\frac{c_j}{(1-u) - v \sum_{i=1}^{N_c} c_i} = \chi_{\{u<1\}} v^{-1} e^{\beta \mu_j^{\infty}} e^{-\beta q_j \psi}.$$

When x is sufficient far away from the solute, we have $u(x) = 0$, $\psi(x) = 0$ and $c_j(x) = c_j^\infty$ with $j \in \{0, 1, \dots, N_c\}$, where c_0^∞ is the (constant) bulk concentration of the solvent molecule. This implies that $c_j^\infty = c_0^\infty e^{\beta \mu_j^\infty}$, where we have used the relation (3.2).

$$\frac{c_j}{(1-u) - \mathbf{v} \sum_{i=1}^{N_c} c_i} = \chi_{\{u < 1\}} h_j e^{-\beta q_j \psi}, \quad \text{where } h_j = \frac{c_j^\infty}{\mathbf{v} c_0^\infty}. \quad (3.14)$$

Summing over $j = 1, \dots, N_c$, one can find out that

$$\begin{aligned} \sum_{j=1}^{N_c} c_j &= (1-u) \frac{\chi_{\{u < 1\}} \sum_{j=1}^{N_c} h_j e^{-\beta q_j \psi}}{1 + \chi_{\{u < 1\}} \mathbf{v} \sum_{j=1}^{N_c} h_j e^{-\beta q_j \psi}} \\ &= (1-u) \frac{\sum_{j=1}^{N_c} c_j^\infty e^{-\beta q_j \psi}}{\mathbf{v} c_0^\infty + \mathbf{v} \sum_{j=1}^{N_c} c_j^\infty e^{-\beta q_j \psi}}. \end{aligned}$$

Here, we have utilized the relation $(1-u)\chi_{\{u < 1\}} = 1-u$. Note that the above equality implies that

$$1-u - \mathbf{v} \sum_{j=1}^{N_c} c_j = \frac{(1-u)\mathbf{v} c_0^\infty}{\mathbf{v} c_0^\infty + \mathbf{v} \sum_{j=1}^{N_c} c_j^\infty e^{-\beta q_j \psi}}.$$

Plugging this expression into (3.2) yields

$$c_j = (1-u) \frac{c_j^\infty e^{-\beta q_j \psi}}{\mathbf{v} c_0^\infty + \mathbf{v} \sum_{i=1}^{N_c} c_i^\infty e^{-\beta q_i \psi}}. \quad (3.15)$$

Using (3.2), the size-modified Helmholtz free energy H_{md} can be reformulated as

$$H_{md} = \int_{\Omega} \left[\rho \psi - \frac{\epsilon(u)}{8\pi} |\nabla \psi|^2 + \beta^{-1} \mathbf{v}^{-1} (1-u) \left(\ln \left(\frac{(1-u)\mathbf{v} c_0^\infty}{\mathbf{v} c_0^\infty + \mathbf{v} \sum_{j=1}^{N_c} c_j^\infty e^{-\beta q_j \psi}} \right) - 1 \right) \right] dx.$$

A constant term (with respect to fixed u)

$$\beta^{-1} \mathbf{v}^{-1} (1-u) \ln \left(\mathbf{v} c_0^\infty + \mathbf{v} \sum_{j=1}^{N_c} c_j^\infty \right) - \beta^{-1} \mathbf{v}^{-1} (1-u) [\ln((1-u)\mathbf{v} c_0^\infty) - 1] \quad (3.16)$$

needs to be added to H_{md} to adjust the reference state of the zero energy in the grand canonical ensemble under consideration. We finally arrive at the following size-modified polar energy functional:

$$I_{p,md}(u, \psi) = \int_{\Omega} \left[\rho \psi - \frac{\epsilon(u)}{8\pi} |\nabla \psi|^2 - (1-u) B_{md}(\psi) \right] dx,$$

where the function $B_{md} : \mathbb{R} \rightarrow \mathbb{R}$ is defined by

$$B_{md}(s) = \beta^{-1} \mathbf{v}^{-1} \ln \left(\frac{\mathbf{v} c_0^\infty + \mathbf{v} \sum_{j=1}^{N_c} c_j^\infty e^{-\beta q_j s}}{\mathbf{v} c_0^\infty + \mathbf{v} \sum_{j=1}^{N_c} c_j^\infty} \right).$$

Direct computations show

$$B'_{md}(s) = - \frac{\sum_{j=1}^{N_c} c_j^\infty q_j e^{-\beta q_j s}}{\mathbf{v} c_0^\infty + \mathbf{v} \sum_{j=1}^{N_c} c_j^\infty e^{-\beta q_j s}}$$

and

$$B''_{md}(s) = \frac{\mathbf{v} \beta c_0^\infty \sum_{j=1}^{N_c} c_j^\infty q_j^2 e^{-\beta q_j s} + \mathbf{v} \beta \left(\sum_{j=1}^{N_c} c_j^\infty q_j^2 e^{-\beta q_j s} \right) \left(\sum_{j=1}^{N_c} c_j^\infty e^{-\beta q_j s} \right) - \mathbf{v} \beta \left(\sum_{j=1}^{N_c} c_j^\infty q_j e^{-\beta q_j s} \right)^2}{\left(\mathbf{v} c_0^\infty + \mathbf{v} \sum_{j=1}^{N_c} c_j^\infty e^{-\beta q_j s} \right)^2}.$$

The Cauchy-Schwartz inequality shows that $B''_{md}(s) > 0$ for all $s \in \mathbb{R}$. Therefore, B_{md} is strictly convex. It follows from (2.2) that $B'_{md}(0) = 0$ and thus $0 = B_{md}(0) = \min_{s \in \mathbb{R}} B_{md}(s)$. Plugging (3.2) into (3) gives the size-modified PB equation

$$\nabla \cdot [\epsilon(u) \nabla \psi] - 4\pi(1-u) B'_{md}(\psi) + 4\pi \rho = 0 \quad \text{in } \Omega. \quad (3.17)$$

Lemma A.1 shows that, for any fixed $u \in \mathcal{X}$, $\psi \in \mathcal{A}$ solves (3.2) iff it maximizes $I_{p,md}(u, \cdot)$.

Define $\mathsf{L}_{md} : \mathcal{X} \rightarrow \mathbb{R}$ by

$$\mathsf{L}_{md}(u) = \int_{\Omega} [P_h u + \rho_s(1-u)U^{\text{vdW}}] dx + I_{p,md}(u, \psi_u),$$

where ψ_u maximizes $I_{p,md}(u, \cdot)$ in \mathcal{A} . Following the proof of Lemma 3.2, we can prove a similar result for L_{md} .

Lemma 3.4. *Let $\{D_k\}_{k \in \mathcal{K}}$ be a family of Caccioppoli sets satisfying $\Omega_i \subset D_k \subset \Omega \setminus \bar{\Omega}_e$ and $p_k \in [0, 1]$ with $\sum_{k \in \mathcal{K}} p_k = 1$. Then for each $\varepsilon > 0$, there exists another family $\{\tilde{D}_k\}_{k \in \mathcal{K}}$ of Caccioppoli sets satisfying $\Omega_i \subset \tilde{D}_k \subset \Omega \setminus \bar{\Omega}_e$ and*

$$\mathcal{H}^2(\partial^* \tilde{D}_k \cap \partial^* \tilde{D}_j) = 0, \quad \forall k, j \in \mathcal{K}, k \neq j.$$

Moreover,

$$\left| \sum_{k \in \mathcal{K}} p_k \int_{\Omega} \theta d|D\chi_{D_k}| + \mathsf{L}_{md}(u) - \sum_{k \in \mathcal{K}} p_k \int_{\Omega} \theta d|D\chi_{\tilde{D}_k}| - \mathsf{L}_{md}(\tilde{u}) \right| < \varepsilon,$$

where $u = \sum_{k \in \mathcal{K}} p_k \chi_{D_k}$ and $\tilde{u} = \sum_{k \in \mathcal{K}} p_k \chi_{\tilde{D}_k}$.

By virtue of Lemma 3.4 and Proposition 3.3, the size-modified EASE functional can be expressed as

$$\mathcal{E}_{md}(u) = \int_{\Omega} \theta d|Du| + \int_{\Omega} \left[P_h u + (1-u) (\rho_s U^{\text{vdW}} - B_{md}(\psi)) + \rho\psi - \frac{\epsilon(u)}{8\pi} |\nabla \psi|^2 \right] dx \quad (3.18)$$

with admissible set \mathcal{X} and $\psi = \psi_u \in \mathcal{A}$ solves the size-modified PB equation (3.2).

4. ANALYSIS OF ENSEMBLE AVERAGE SOLVATION ENERGY

We will perform some preliminary analysis for the EASE models developed in the previous section. The following example shows that \mathcal{E} is not l.s.c. with respect to convergence in $W^{1,1}(\Omega)$.

Example 4.1. *We take $\psi_D \equiv 1$, $\Omega_i = B(0, 1)$, $\Omega_t = \{x \in \mathbb{R}^3 : 1 < |x| < 2\}$ and $\Omega_e = \{x \in \mathbb{R}^3 : 2 < |x| < 3\}$. Choose $u \in \mathcal{X} \cap C^\infty(\Omega)$ such that $u(x) = 1$ for $|x| \leq \frac{5}{3}$ and $u(x) < 1$ elsewhere. We can construct a sequence $u_n \in \mathcal{X} \cap W^{1,1}(\Omega)$ such that $u_n \rightarrow u$ in $W^{1,1}(\Omega)$ satisfying*

- $u_n(x) < 1$ for all $|x| > 1$,
- $u_n(x) = \frac{n-1}{n}$ for $\frac{4}{3} \leq |x| \leq \frac{5}{3}$.

For instance, we can define $u_n(x) = \frac{n+3}{n} - \frac{3}{n}|x|$ for $1 \leq |x| \leq \frac{4}{3}$ and $u_n(x) = \frac{n-1}{n}u(x)$ for $|x| > \frac{4}{3}$. Direct computations show that

$$\lim_{n \rightarrow \infty} I_{np}(u_n) = I_{np}(u).$$

However, Lemma A.2 shows that

$$\lim_{n \rightarrow \infty} I_p(u_n, \psi_{u_n}) = \int_{\Omega} \left[\rho\psi_* - \frac{\epsilon(u)}{8\pi} |\nabla \psi_*|^2 - \chi_{\{|x|>1\}} B(\psi_*) \right] dx \leq I_p(u, \psi_*) \leq I_p(u, \psi_u), \quad (4.1)$$

where $\psi_u \in \mathcal{A}$ is the solution of (3.1.1) and ψ_{u_n} is the solution with u replaced by u_n . Additionally, ψ_* is the solution of

$$\nabla \cdot [\epsilon(u) \nabla \psi] - 4\pi \chi_{\{|x|>1\}} B'(\psi) + 4\pi \rho = 0 \quad \text{in } \Omega.$$

Note that equalities hold in (4.1) iff $\psi_u = \psi_*$ and $\psi_*(x) = 0$ for a.a. $1 < |x| \leq \frac{5}{3}$. If the second condition holds, then ψ_* solves

$$\begin{cases} \nabla \cdot [\epsilon(u) \nabla \psi] - 4\pi B'(\psi) = 0 & \text{in } \{1 < |x| < 3\}, \\ \psi = 0 & \text{on } \{|x| = 1\}, \\ \psi = 1 & \text{on } \partial\Omega. \end{cases}$$

Then it follows from the elliptic unique continuation theorem, c.f. [17, Theorem 1.4], that $\psi_* \equiv 0$, which contradicts with the fact that $\psi_* = 1$ on $\partial\Omega$.

The analysis above reveals that the absence of lower semicontinuity in \mathcal{E} arises from the discontinuous term $\chi_{\{u < 1\}}$. Minimizing non-lower semicontinuous functionals poses a significant challenge. Particularly, the computational and analytical complexities associated with the discontinuous term further compound the difficulty. Consequently, the minimization of \mathcal{E} remains an open problem.

In contrast, the discontinuous term $\chi_{\{u < 1\}}$ is obviated in \mathcal{E}_{md} through the relation $(1 - u)\chi_{\{u < 1\}} = 1 - u$. This elimination allows us to establish the lower semicontinuity of \mathcal{E}_{md} , as demonstrated in the proof of Theorem 4.2 below. This paves the way for establishing additional analytic properties of \mathcal{E}_{md} . Consequently, our focus in the remainder of this article will center on the analysis of the size-modified EASE functional \mathcal{E}_{md} . The analyses in the following two subsections underscore the advantages of incorporating finite size effects in EASE modeling from an analytical perspective.

4.1. Existence of Minimizer.

Theorem 4.2. \mathcal{E}_{md} has a global minimizer in \mathcal{X} .

Proof. First, we will show that \mathcal{E}_{md} is convex. Indeed, given any $u_0, u_1 \in \mathcal{X}$, let $u_t = tu_0 + (1 - t)u_1$ for $t \in [0, 1]$. We have $u_t \in \mathcal{X}$ for all $t \in [0, 1]$. For any $v \in \mathcal{X}$, let ψ_v be the solution of (3.2) in \mathcal{A} with u replaced by v . Note that, for any fixed $\psi \in \mathcal{A}$, both $I_{np}(\cdot)$ and $I_{p,md}(\cdot, \psi)$ are convex. Then it follows from Lemma A.1 that

$$\begin{aligned} \mathcal{E}_{md}(u_t) &= I_{np}(u_t) + I_{p,md}(u_t, \psi_{u_t}) \\ &\leq t [I_{np}(u_0) + I_{p,md}(u_0, \psi_{u_t})] + (1 - t) [I_{np}(u_1) + I_{p,md}(u_1, \psi_{u_t})] \\ &\leq t [I_{np}(u_0) + I_{p,md}(u_0, \psi_{u_0})] + (1 - t) [I_{np}(u_1) + I_{p,md}(u_1, \psi_{u_1})] \\ &= t\mathcal{E}(u_0) + (1 - t)\mathcal{E}(u_1). \end{aligned}$$

The lower semicontinuity of \mathcal{E}_{md} in \mathcal{X} with respect to convergence in $L^1(\Omega)$ is a direct conclusion from the dominated convergence theorem, [10, Corollary 1], and Lemma A.2. Now the existence of a minimizer of \mathcal{E}_{md} in \mathcal{X} can be immediately obtained by the direct method of Calculus of Variation. \square

Remark 4.3. The assertion of Theorem 4.2 remains valid if we merely assume that Σ_0 and Σ_1 are Lipschitz continuous.

4.2. Continuous dependence on the constraints. Let $\mathcal{E} = \min_{u \in \mathcal{X}} \mathcal{E}_{md}(u)$. Since \mathcal{E} depends on Constraint (3) and thus on Σ_0 and Σ_1 , we will justify the robustness of (3.2) by demonstrating that \mathcal{E} depends continuously on Σ_j with $j = 0, 1$ in a proper topology. Without loss of generality, we may assume that Σ_j are connected. The general case can be proved in a similar manner.

For $k = 1, 2$, let \mathcal{MH}^k be the set of pairs (Σ_0, Σ_1) of compact, connected and oriented C^k -hypersurfaces without boundary contained in the open set Ω , which induces a decomposition $(\Omega_i, \Omega_t, \Omega_e)$ as in Figure 1(B). The orientation of Σ_0 (Σ_1 , resp.) is so taken that its outward unit normal vector field ν_{Σ_0} (ν_{Σ_1} , resp.) points into Ω_t . To summarize, the open sets $(\Omega_i, \Omega_t, \Omega_e)$ satisfy the following properties.

- $(\Omega_i, \Omega_t, \Omega_e)$ are connected so that $\Sigma_0 \cap \Sigma_1 = \emptyset$.
- $\bigcup_{i=1}^{N_m} \overline{B}(x_i, \sigma_i) \subset \Omega_i \Subset \Omega \setminus \overline{\Omega}_e$.
- $\partial\Omega \subset \partial\Omega_e$.

Theorem 4.2 and Remark 4.3 show that \mathcal{E} can be considered a functional defined on \mathcal{MH}^1 . In the rest of this section, we denote \mathcal{E}_{md} , \mathcal{X} , and $(\Omega_i, \Omega_t, \Omega_e)$ by $\mathcal{E}_{md,\Gamma}$, \mathcal{X}_Γ , and $(\Omega_{i,\Gamma}, \Omega_{t,\Gamma}, \Omega_{e,\Gamma})$ to indicate their dependence on $\Gamma = (\Sigma_0, \Sigma_1) \in \mathcal{MH}^1$. In Theorem 4.4 below, it will be shown that \mathcal{E} is indeed continuous while restricted to \mathcal{MH}^2 . To this end, we will first demonstrate that \mathcal{MH}^k are metric spaces.

The normal bundle of a compact, connected and oriented C^1 -hypersurface Σ without boundary is given by

$$\mathcal{N}^1\Sigma = \{(\mathbf{q}, \nu_\Sigma(\mathbf{q})) : \mathbf{q} \in \Sigma\} \subset \mathbb{R}^3 \times \mathbb{R}^3,$$

where $\nu_\Sigma(\mathbf{q})$ is the outward unit normal of Σ at $\mathbf{q} \in \Sigma$. If in addition, Σ is C^2 , its second normal bundle can be defined as

$$\mathcal{N}^2\Sigma = \{(\mathbf{q}, \nu_\Sigma(\mathbf{q}), \nabla_\Sigma \nu_\Sigma(\mathbf{q})) : \mathbf{q} \in \Sigma\} \subset \mathbb{R}^3 \times \mathbb{R}^3 \times \mathbb{R}^6,$$

where ∇_Σ is the surface gradient of Σ . Recall that the Hausdorff metric on compact subsets $K \subset \mathbb{R}^n$ is defined by

$$d_{\mathcal{H}}(K_1, K_2) = \max\left\{\sup_{x \in K_1} d(x, K_2), \sup_{x \in K_2} d(x, K_1)\right\}.$$

We can equip \mathcal{MH}^k with the metric

$$d_{\mathcal{MH}^k}((\Sigma_0, \Sigma_1), (\tilde{\Sigma}_0, \tilde{\Sigma}_1)) = d_{\mathcal{H}}(\mathcal{N}^k \Sigma_0, \mathcal{N}^k \tilde{\Sigma}_0) + d_{\mathcal{H}}(\mathcal{N}^k \Sigma_1, \mathcal{N}^k \tilde{\Sigma}_1), \quad (\Sigma_0, \Sigma_1), (\tilde{\Sigma}_0, \tilde{\Sigma}_1) \in \mathcal{MH}^k.$$

Following [43, Chapter 2], one can show that \mathcal{MH}^2 equipped with $d_{\mathcal{MH}^2}$ is a Banach manifold. The theorem below is the main result of this section.

Theorem 4.4. $\mathcal{E} \in C(\mathcal{MH}^2)$.

We will split the proof of Theorem 4.4 into several steps. Pick arbitrary $\Gamma = (\Sigma_0, \Sigma_1) \in \mathcal{MH}^2$. To prove the continuity of \mathcal{E} at Γ , we choose an arbitrary sequence $\Gamma_n := (\Sigma_{0,n}, \Sigma_{1,n}) \in \mathcal{MH}^1$. In the sequel, we will first prove two propositions concerning the convergence $\lim_{n \rightarrow \infty} \mathcal{E}(\Gamma_n) = \mathcal{E}(\Gamma)$ under the condition

$$\lim_{n \rightarrow \infty} d_{\mathcal{MH}^1}(\Gamma_n, \Gamma) = 0 \quad (4.2)$$

when Γ_n converges to Γ from the interior and exterior of Γ (with respect to the orientations of (Σ_0, Σ_1)). In the rest of this section, we will denote by u_{\min} ($u_{\min;n}$, resp.) a global minimizer of $\mathcal{E}_{md,\Gamma}$ ($\mathcal{E}_{md,\Gamma_n}$ resp.) in \mathcal{X}_{Γ} (\mathcal{X}_{Γ_n} resp.).

Proposition 4.5. Assume that $\Gamma = (\Sigma_0, \Sigma_1) \in \mathcal{MH}^2$ and $\Gamma_n = (\Sigma_{0,n}, \Sigma_{1,n}) \in \mathcal{MH}^1$ satisfy (4.2). If

$$\Omega_{i,\Gamma_n} \subset \Omega_{i,\Gamma} \quad \text{and} \quad \Omega_{e,\Gamma_n} \subset \Omega_{e,\Gamma},$$

then $\lim_{n \rightarrow \infty} \mathcal{E}(\Gamma_n) = \mathcal{E}(\Gamma)$.

Proof. Observe that $u_{\min} \in \mathcal{X}_{\Gamma_n}$ for all n . Thus

$$\mathcal{E}(\Gamma_n) = \mathcal{E}_{md,\Gamma_n}(u_{\min;n}) \leq \mathcal{E}_{md,\Gamma_n}(u_{\min}) = \mathcal{E}_{md,\Gamma}(u_{\min}) = \mathcal{E}(\Gamma).$$

It follows from Lemma A.1 that there exists some constant $M > 0$ such that

$$\left| \int_{\Omega} \rho_s U^{\text{vdW}}(1 - u_{\min;n}) dx + I_{p,md}(u_{\min;n}, \psi_{u_{\min;n}}) \right| \leq M,$$

where $\psi_{u_{\min;n}} \in \mathcal{A}$ is the solution of (3.2) with u replaced by $u_{\min;n}$. This implies that

$$\theta_0 \int_{\Omega} d|Du_{\min;n}| + P_h \|u_{\min;n}\|_{L^1} - M \leq \mathcal{E}(\Gamma).$$

Therefore, $\|u_{\min;n}\|_{BV}$ is uniformly bounded. [24, Theorem 5.2.3.4] implies that there exists a subsequence, not relabelled, and some $u \in BV(\Omega)$ such that $u_{\min;n} \rightarrow u$ in $L^1(\Omega)$. Note that (4.2) implies that

$$\lim_{n \rightarrow \infty} \|\chi_{\Omega_{i,\Gamma_n}} - \chi_{\Omega_{i,\Gamma}}\|_{L^1} = \lim_{n \rightarrow \infty} \|\chi_{\Omega_{e,\Gamma_n}} - \chi_{\Omega_{e,\Gamma}}\|_{L^1} = 0$$

and thus $u \in \mathcal{X}_{\Gamma}$. From [10, Corollary 1], Lemma A.2 and the dominated convergence theorem, we infer that

$$\mathcal{E}(\Gamma) \leq \mathcal{E}_{md,\Gamma}(u) \leq \liminf_{n \rightarrow \infty} \mathcal{E}(\Gamma_n) \leq \limsup_{n \rightarrow \infty} \mathcal{E}(\Gamma_n) \leq \mathcal{E}(\Gamma).$$

This proves the assertion. \square

To prove the convergence $\lim_{n \rightarrow \infty} \mathcal{E}(\Gamma_n) = \mathcal{E}(\Gamma)$ in case

$$\Omega_{i,\Gamma_n} \supseteq \Omega_{i,\Gamma} \quad \text{and} \quad \Omega_{e,\Gamma_n} \supseteq \Omega_{e,\Gamma},$$

we will need some preparations. Because Σ_i are C^2 , following the proof of Lemma 3.2, the map

$$\Lambda_i : \Sigma_i \times (-\mathbf{a}, \mathbf{a}) \rightarrow B_{\mathbf{a}}(\Sigma_i) : (\mathbf{q}, r) \mapsto \mathbf{q} + r\nu_{\Sigma_i}(\mathbf{q}), \quad i = 0, 1,$$

is a C^1 -diffeomorphism for some $\mathbf{a} > 0$, where $B_{\mathbf{a}}(\Sigma_i)$ is the tubular neighbourhood of Σ_i with width \mathbf{a} and ν_{Σ_i} is the outward unit normal of Σ_i . By the inverse function theorem, there exist two maps $P_i \in C^1(B_{\mathbf{a}}(\Sigma_i), \Sigma_i)$ and $d_i \in C^1(B_{\mathbf{a}}(\Sigma_i), (-\mathbf{a}, \mathbf{a}))$, where P_i is the nearest point projection onto Σ_i and d_i is the signed distance to Σ_i with $d_i(x) > 0$ for $x \in B_{\mathbf{a}}(\Sigma_i) \cap \Omega_t$. Note that $\mathcal{G}_i^r := \Lambda_i(\Sigma_i, r) \in \mathcal{MH}^1$. Its orientation is chosen to be compatible with that of Σ_i so that its outward unit normal

$$\nu_{i,r}(x) = \nu_{\Sigma_i}(P_i(x)), \quad x \in \mathcal{G}_i^r.$$

See [43, Section 2.2.2]. Then it is clear that $\lim_{r \rightarrow 0} d_{\mathcal{H}}(\mathcal{G}_i^r, \Sigma_i) = 0$. Without loss of generality, we may assume that $\mathbf{a} > 0$ is so small that for any $r \in (-\mathbf{a}, \mathbf{a})$, $\mathcal{G}_0^r \cap \mathcal{G}_1^r = \emptyset$.

Lemma 4.6. *For every $f \in \mathcal{X}_\Gamma$, we define*

$$f_r(x) = \begin{cases} 1, & x \in \Omega_i \cup B_r(\Sigma_1) \\ 0, & x \in \Omega_e \cup B_r(\Sigma_0) \\ f(x), & \text{elsewhere} \end{cases}$$

for $r \in (0, a)$. Then $f_r \rightarrow f$ in $L^1(\Omega)$ and $\int_\Omega \theta d|Df_r(x)| \rightarrow \int_\Omega \theta d|Df(x)|$ as $r \rightarrow 0^+$.

Proof. The proof for $f_r \rightarrow f$ in $L^1(\Omega)$ is straightforward. So we will only show the second part. [10, Corollary 1] implies that $\int_\Omega \theta d|Df(x)| \leq \liminf_{r \rightarrow 0^+} \int_\Omega \theta d|Df_r(x)|$. In the rest of the proof, it is assumed that $i \in \{0, 1\}$. Put $U_i^r := B_r(\Sigma_i) \cap \Omega_i$. For any $\phi \in C_c^1(\Omega; \mathbb{R}^3)$ with $\|\phi\|_\infty \leq 1$ and $u \in \mathcal{X}_\Gamma$, the trace theorem of BV-functions, cf. [24, Theorem 5.3.1] implies that

$$\int_{U_i^r} u \nabla \cdot (\theta \phi) dx + \int_{U_i^r} (\theta \phi) \cdot d[Du] = \int_{\mathcal{G}_i^r} (\theta \phi) \cdot \nu_{i,r} T_r u d\mathcal{H}^2 - \int_{\Sigma_i} (\theta \phi) \cdot \nu_{\Sigma_i} T_r u d\mathcal{H}^2.$$

Here $T_r u$ is the trace of $u|_{U_i^r}$ on ∂U_i^r ; and $[Du]$ is the vector-valued measure for the gradient of u . Pushing $r \rightarrow 0^+$ above yields that

$$\lim_{r \rightarrow 0^+} \int_{\mathcal{G}_i^r} (\theta \phi) \cdot \nu_{i,r} T_r u d\mathcal{H}^2 = \int_{\Sigma_i} (\theta \phi) \cdot \nu_{\Sigma_i} T_r u d\mathcal{H}^2. \quad (4.3)$$

Direct computations show

$$\begin{aligned} \int_\Omega (\theta \phi) \cdot d[Df_r] &= \sum_{i=0,1} \int_{\mathcal{G}_i^r} (\theta \phi) \cdot d[Df_r] + \int_{\Omega \setminus (U_0^r \cup U_1^r)} (\theta \phi) \cdot d[Df] \\ &= \int_\Omega (\theta \phi) \cdot d[Df] - \sum_{i=0,1} \int_{U_i^r} (\theta \phi) \cdot d[Df] - \sum_{i=0,1} \int_{\Sigma_i} (\theta \phi) \cdot d[Df] \\ &\quad - \sum_{i=0,1} \int_{\mathcal{G}_i^r} (\theta \phi) \cdot d[D(f - f_r)] \\ &\leq \int_\Omega \theta d|Df(x)| - \sum_{i=0,1} \int_{U_i^r} (\theta \phi) \cdot d[Df] - \sum_{i=0,1} \int_{\Sigma_i} (\theta \phi) \cdot d[Df] \\ &\quad - \sum_{i=0,1} \int_{\mathcal{G}_i^r} (\theta \phi) \cdot d[D(f - f_r)]. \end{aligned}$$

It follows from (4.2) that

$$\begin{aligned} & - \sum_{i=0,1} \int_{\Sigma_i} (\theta \phi) \cdot d[Df] - \sum_{i=0,1} \int_{\mathcal{G}_i^r} (\theta \phi) \cdot d[D(f - f_r)] \\ &= \sum_{i=0,1} \int_{\Sigma_i} (\theta \phi) \cdot \nu_{\Sigma_i} (i - T_r f) d\mathcal{H}^2 - \sum_{i=0,1} \int_{\mathcal{G}_i^r} (\theta \phi) \cdot \nu_{i,r} (i - T_r f) d\mathcal{H}^2 \rightarrow 0 \end{aligned}$$

as $r \rightarrow 0^+$. See the proof of [24, Theorem 5.4.1]. We clearly have $\lim_{r \rightarrow 0^+} \int_{U_i^r} (\theta \phi) \cdot d[Df] = 0$. Therefore, we can infer from (2.2) and [24, Theorem 5.3.1] that

$$\limsup_{r \rightarrow 0^+} \int_\Omega \theta d|Df_r(x)| \leq \int_\Omega \theta d|Df(x)|.$$

This proves the assertion □

Proposition 4.7. *Assume that $\Gamma = (\Sigma_0, \Sigma_1) \in \mathcal{MH}^2$ and $\Gamma_n = (\Sigma_{0,n}, \Sigma_{1,n}) \in \mathcal{MH}^1$ satisfy (4.2). If*

$$\Omega_{i,\Gamma_n} \supseteq \Omega_{i,\Gamma} \quad \text{and} \quad \Omega_{e,\Gamma_n} \supseteq \Omega_{e,\Gamma},$$

then $\lim_{n \rightarrow \infty} \mathcal{E}(\Gamma_n) = \mathcal{E}(\Gamma)$.

Proof. Let $r_n = d_{\mathcal{MH}^1}(\Gamma_n, \Gamma)$. For sufficiently large $n \in \mathbb{N}$, we define

$$u_n(x) = \begin{cases} 1, & x \in \Omega_i \cup B_{r_n}(\Sigma_1), \\ 0, & x \in \Omega_e \cup B_{r_n}(\Sigma_0), \\ u_{\min}(x), & \text{elsewhere.} \end{cases}$$

Since $u_n \in \mathcal{X}_{\Gamma_n}$ and $u_{\min;n} \in \mathcal{X}_{\Gamma}$, we have

$$\mathcal{E}(\Gamma) \leq \mathcal{E}_{md,\Gamma}(u_{\min;n}) = \mathcal{E}_{md,\Gamma_n}(u_{\min;n}) = \mathcal{E}(\Gamma_n) \leq \mathcal{E}_{md,\Gamma_n}(u_n) = \mathcal{E}_{md,\Gamma}(u_n). \quad (4.4)$$

Lemma 4.6 implies that as $n \rightarrow \infty$

$$u_n \rightarrow u_{\min} \quad \text{in } L^1(\Omega) \quad \text{and} \quad \int_{\Omega} \theta d|Du_n| \rightarrow \int_{\Omega} \theta d|Du_{\min}|.$$

Using the dominated convergence theorem and Lemma A.2 yields $\lim_{n \rightarrow \infty} \mathcal{E}_{md,\Gamma}(u_n) = \mathcal{E}_{md,\Gamma}(u_{\min}) = \mathcal{E}(\Gamma)$. Then the asserted statement follows by pushing $n \rightarrow \infty$ in (4.2). \square

Proof of Theorem 4.4. Now we assume that $\Gamma_n \in \mathcal{MH}^2$ and

$$\Gamma_n := (\Sigma_{0,n}, \Sigma_{1,n}) \rightarrow \Gamma \quad \text{in } \mathcal{MH}^2.$$

Let $r_n = d_{\mathcal{MH}^2}(\Gamma_n, \Gamma)$. Then $\mathcal{G}^{\pm r_n} = (\mathcal{G}_0^{\pm r_n}, \mathcal{G}_1^{\pm r_n}) \in \mathcal{MH}^1$. We denote by u_n^{\pm} a global minimizer of $\mathcal{E}_{md,\mathcal{G}^{\pm r_n}}$ in $\mathcal{X}_{\mathcal{G}^{\pm r_n}}$. Because $u_{\min;n} \in \mathcal{X}_{\mathcal{G}^{-r_n}}$ and $u_n^+ \in \mathcal{X}_{\Gamma_n}$, we infer that

$$\mathcal{E}(\mathcal{G}^{-r_n}) \leq \mathcal{E}_{md,\mathcal{G}^{-r_n}}(u_{\min;n}) = \mathcal{E}_{md,\Gamma_n}(u_{\min;n}) = \mathcal{E}(\Gamma_n) \leq \mathcal{E}_{md,\Gamma_n}(u_n^+) = \mathcal{E}_{md,\mathcal{G}^{+r_n}}(u_n^+) = \mathcal{E}(\mathcal{G}^{+r_n}).$$

Propositions 4.5 and 4.7 show that

$$\lim_{n \rightarrow \infty} \mathcal{E}(\mathcal{G}^{-r_n}) = \lim_{n \rightarrow \infty} \mathcal{E}(\mathcal{G}^{+r_n}) = \mathcal{E}(\Gamma).$$

Therefore, $\lim_{n \rightarrow \infty} \mathcal{E}(\Gamma_n) = \mathcal{E}(\Gamma)$. \square

5. CONCLUSION

Variational implicit solvation models (VISM) have been successful in the computation of solvation energies. However, traditional sharp-interface VISMs do not account for the inherent randomness of the solute-solvent interface, stemming from thermodynamic fluctuations. It has been demonstrated that neglecting these fluctuations can lead to substantial errors in predicting solvation free energies.

In this work, a new approach to calculating ensemble averaged solvation energy (EASE) is developed using diffuse-interface VISM. Grounded in principles of statistical mechanics and geometric measure theory, the method effectively captures EASE during the solvation process by employing a novel diffuse-interface profile $u(x)$, which represents the probability of finding a point x in the solute phase across all microstates within the grand canonical ensemble. To showcase the versatility of our modeling paradigm, we formulate two EASE functionals: one within the classic Poisson-Boltzmann (PB) framework and another within the framework of size-modified PB theory, accounting for finite-size effects of mobile ions and solvent molecules.

In the routine calculation of the EASE, one needs to carry out molecular dynamics (MD) simulations to obtain thousands of solute-solvent configurations (snapshots) and perform energy calculations for each snapshot. By meticulously modeling the impact of conformational changes in the solvent medium, the proposed model can reproduce EASE with just one diffuse-interface configuration, potentially drastically speeding up calculations compared to ensemble-averaging energies from thousands of snapshots.

Preliminary analyses of the proposed EASE models indicate that the size-modified EASE functional outperforms the EASE functional in the classic PB theory in various analytical aspects. Motivated by these observations, we plan to conduct numerical implementations and further theoretical analyses of the size-modified EASE functional in future work.

APPENDIX A. A CLASS OF STRICTLY CONVEX FUNCTIONALS

In this section, we collect some results concerning a class of strictly convex functionals associated with the polar solvation energy. These results can be proved by following the proofs of [14, Propositions 3.1 and 3.2] line by line. We will thus omit their proofs.

Throughout this appendix, we assume that $F \in C^\infty(\mathbb{R})$ is a strictly convex function with $F'(0) = 0$ and $F(0) = 0$.

Lemma A.1. *Assume that $a, b, c \in L^\infty(\Omega)$ satisfy*

$$0 < L_0 \leq a \leq L_1, \quad 0 \leq b \leq L_2, \quad \|c\|_\infty \leq L_3 \quad (\text{A.1})$$

for some constants L_i . Then the functional

$$G(\psi) = \int_{\Omega} \left[\frac{a}{2} |\nabla \psi|^2 + bF(\psi) - c\psi \right] dx$$

has a unique minimizer $\psi \in \mathcal{A}$ for every $\psi_D \in W^{1,\infty}(\Omega)$, c.f. (2.2), or equivalently, ψ weakly solves

$$\begin{cases} \nabla \cdot (a \nabla \psi) - bF'(\psi) + c = 0 & \text{in } \Omega; \\ \psi = \psi_D & \text{on } \partial\Omega. \end{cases}$$

Moreover, for some constant C_∞ depending only on L_i and ψ_D

$$\|\psi\|_{H^1} + \|\psi\|_{L^\infty} \leq C_\infty.$$

Lemma A.2. *Let $a_n, b_n, c \in L^\infty(\Omega)$ satisfy (A.1), $n = 0, 1, \dots$. Assume that ψ_n is the unique minimizer of*

$$G_n(\psi) = \int_{\Omega} \left[\frac{a_n}{2} |\nabla \psi|^2 + b_n F(\psi) - c\psi \right] dx$$

in \mathcal{A} for some $\psi_D \in W^{1,\infty}(\Omega)$. If $a_n \rightarrow a_0$ and $b_n \rightarrow b_0$ in $L^1(\Omega)$ as $n \rightarrow \infty$, then

$$\psi_n \rightarrow \psi_0 \quad \text{in } H^1(\Omega), \quad \text{and} \quad \lim_{n \rightarrow \infty} G_n(\psi_n) = G_0(\psi_0).$$

APPENDIX B. A COMPARISON WITH GFBVISM

In this section, we will conduct a comparative analysis of the proposed models (3.1.3) and (3.2) with a closely related VISM known as the Geometric Flow-Based VISM (GFBVISM), which is rooted in classic PB theory. GFBVISM [13] is defined as follows:

$$\mathcal{E}^{(2)}(u) = I_{\text{np}}(u) + I_{\text{p}}^{(2)}(u, \psi), \quad (\text{B.1})$$

where

$$I_{\text{p}}^{(2)}(u, \psi) = \int_{\Omega} \left[\rho\psi - \frac{\epsilon(u)}{8\pi} |\nabla \psi|^2 - (1-u)B(\psi) \right] dx, \quad (\text{B.2})$$

and $\psi \in \mathcal{A}$ solves

$$\nabla \cdot [\epsilon(u) \nabla \psi] - 4\pi(1-u)B'(\psi) + 4\pi\rho = 0 \quad \text{in } \Omega. \quad (\text{B.3})$$

Despite certain similarities between (3.1.3) and (3.2) and GFBVISM, there exist fundamental distinctions between them.

First, (B) was introduced in an *ad hoc* way to create a transition region between the solute and solvent, lacking an explanation of the physical meanings of the transition parameter u and the predicted energy.

Second, it has come to attention that the original formulation of GFBVISM [13] does not incorporate Constraints (3) and (3). This absence of constraints introduces the possibility of nonphysical minimizers within the GFBVISM model. For instance, it may allow for trivial values of u or even negative values, which are not physically meaningful in the given context. Therefore, including these constraints becomes crucial to ensure the model's solutions align with physical principles.

Third and most importantly, the proposed models correct and improve the derivation of the ensemble average polar energy. Due to Proposition 3.1, one may guess that $I_{\text{p}}^{(2)}$ approximates the ensemble average

polar energy. However, Formulation (B) is questionable in the sense that it is derived from an erroneous “entropy” formulation. To see this, on a heuristic level, one can ensemble average the entropy and obtain

$$-T\langle S \rangle = -T \sum_{k \in \mathcal{K}} p_k S_k = \beta^{-1} \sum_{k \in \mathcal{K}} p_k \int_{\Omega} \sum_{j=1}^{N_c} c_j^k [\ln(v c_j^k) - 1] dx \quad \text{and} \quad \langle H \rangle := \langle E \rangle - T\langle S \rangle,$$

where S_k is defined in (2.1). By taking the first variations of $\langle H \rangle$ with respect to all c_j^k , a similar argument to Remark 2.1 gives (2.1). It follows from (3) that

$$c_j(x) = \sum_{k \in \mathcal{K}} p_k c_j^k(x) = \sum_{k \in \mathcal{K}} p_k \chi_{U_k}(x) c_j^k(x) = (1 - u(x)) c_j^{\infty} e^{-\beta q_j \psi(x)}. \quad (\text{B.4})$$

See (2.1) for the definition of S_k . Plugging (B) into (2.1) yields (B). Using the expression (B) of c_j in $\langle H \rangle$ and adding a constant term $\beta^{-1} \sum_{j=1}^{N_c} c_j^{\infty} \int_{\Omega} (1 - u) dx$ to adjust the state of zero energy as in (3.2) give the polar energy formulation (B). From a statistical mechanics perspective, it is indeed important to note that the choice of the “entropy” $\langle S \rangle$ and “Helmholtz free energy” $\langle H \rangle$ in the previous derivation is incorrect. Consequently, (3.1.3) corrects the polar energy formulation within the classical PB theory framework, albeit introducing a discontinuous term $\chi_{\{u < 1\}}$. It is crucial to adhere to the correct statistical mechanics principles when formulating the ensemble averages. Moreover, (3.2) further refines the EASE formulation by accounting for the finite size effects and eliminate the discontinuous term $\chi_{\{u < 1\}}$.

FUNDING INFORMATION

This research was partially supported by the National Science Foundation under grants DMS-2306991 (Shao, Zhao), DMS-1818748 and DMS-2306992 (Chen), DMS-2110914 (Zhao), and a CARSCA grant from the University of Alabama (Shao).

CONFLICT OF INTEREST

The authors declare that they have no known competing financial interests that could have appeared to influence the work reported in this paper. Although Dr. Shan Zhao is a Journal Editor of the Computational and Mathematical Biophysics, he had no involvement in the peer reviewing process or the final decision of this manuscript.

ETHICS STATEMENT

This research does not require ethical approval.

DATA AVAILABILITY STATEMENT

Data sharing is not applicable to this article as no data sets were generated or analysed during the current study.

REFERENCES

- [1] N. A. Baker. Improving implicit solvent simulations: a Poisson-centric view. *Current Opinion in Structural Biology*, 15(2):137–43, 2005.
- [2] N. A. Baker, D. Sept, S. Joseph, M. J. Holst, and J. A. McCammon. Electrostatics of nanosystems: Application to microtubules and the ribosome. *Proceedings of the National Academy of Sciences*, 98(18):10037–10041, 2001.
- [3] P. Ball. How to keep dry in water. *Nature*, 423(6935):25–26, May 2003.
- [4] P. W. Bates, G. W. Wei, and S. Zhao. Minimal molecular surfaces and their applications. *Journal of Computational Chemistry*, 29(3):380–91, 2008.
- [5] J.J. Bikerman. Xxxix. structure and capacity of electrical double layer. *The London, Edinburgh, and Dublin Philosophical Magazine and Journal of Science*, 33(220):384–397, 1942.
- [6] I. Borukhov, D. Andelman, and H. Orland. Adsorption of large ions from an electrolyte solution: a modified poisson-boltzmann equation. *Electrochimica Acta*, 46(2):221–229, 2000.
- [7] Itamar Borukhov, David Andelman, and Henri Orland. Steric effects in electrolytes: A modified poisson-boltzmann equation. *Phys. Rev. Lett.*, 79:435–438, Jul 1997.
- [8] A. H. Boschitsch and M. O. Fenley. Hybrid boundary element and finite difference method for solving the nonlinear Poisson-Boltzmann equation. *Journal of Computational Chemistry*, 25(7):935–955, 2004.
- [9] W. M. Botello-Smith, X. Liu, Q. Cai, Z. Li, H. Zhao, and R. Luo. Numerical poisson-boltzmann model for continuum membrane systems. *Chemical Physics Letters*, 555:274–281, 2013.

- [10] G. Carlier and M. Comte. On a weighted total variation minimization problem. *J. Funct. Anal.*, 250(1):214–226, 2007.
- [11] J. Che, J. Dzubiella, B. Li, and J. A. McCammon. Electrostatic free energy and its variations in implicit solvent models. *The Journal of Physical Chemistry B*, 112(10):3058–3069, 2008. PMID: 18275182.
- [12] C. J. Chen, R. Saxena, and G. W. Wei. Differential geometry based multiscale models for virus formation and evolution. *Int. J. Biomed. Imaging*, 2010(308627), 2010.
- [13] Z. Chen, N. A. Baker, and G. W. Wei. Differential geometry based solvation model I: Eulerian formulation. *J. Comput. Phys.*, 229(22):8231–8258, 2010.
- [14] Z. Chen and Y. Shao. A new approach to constrained total variation solvation models and the study of solute-solvent interface profiles. *Comput. Math. Appl.*, 130:119–136, 2023.
- [15] Z. Chen, S. Zhao, J. Chun, D. G. Thomas, N. A. Baker, P. W. Bates, and G. W. Wei. Variational approach for nonpolar solvation analysis. *The Journal of Chemical Physics*, 137(8):084101, 2012.
- [16] L. T. Cheng, J. Dzubiella, A. J. McCammon, and B. Li. Application of the level-set method to the implicit solvation of nonpolar molecules. *Journal of Chemical Physics*, 127(8), 2007.
- [17] Mourad Choulli. Uniqueness of continuation for semilinear elliptic equations. *arXiv:2208.08378*.
- [18] P. B. Crowley and A. Golovin. Cation- π interactions in protein-protein interfaces. *Proteins: Structure, Function, and Bioinformatics*, 59(2):231–239, 2005.
- [19] S. Dai, B. Li, and J. Lu. Convergence of phase-field free energy and boundary force for molecular solvation. *Arch. Ration. Mech. Anal.*, 227(1):105–147, 2018.
- [20] F. Dong and H. X. Zhou. Electrostatic contribution to the binding stability of protein-protein complexes. *Proteins*, 65(1):87–102, 2006.
- [21] A. I. Dragan, C. M. Read, E. N. Makeyeva, E. I. Milgotina, M. E. Churchill, C. Crane-Robinson, and P. L. Privalov. DNA binding and bending by HMG boxes: Energetic determinants of specificity. *Journal of Molecular Biology*, 343(2):371–393, 2004.
- [22] J. Dzubiella, J. M. J. Swanson, and J. A. McCammon. Coupling hydrophobicity, dispersion, and electrostatics in continuum solvent models. *Phys. Rev. Lett.*, 96:087802, Mar 2006.
- [23] J. Dzubiella, J. M. J. Swanson, and J. A. McCammon. Coupling nonpolar and polar solvation free energies in implicit solvent models. *The Journal of Chemical Physics*, 124(8):084905, 2006.
- [24] L. C. Evans and R. F. Gariepy. *Measure theory and fine properties of functions*. Studies in Advanced Mathematics. CRC Press, Boca Raton, FL, 1992.
- [25] M. Feig and C. L. Brooks III. Recent advances in the development and application of implicit solvent models in biomolecule simulations. *Curr Opin Struct Biol.*, 14:217 – 224, 2004.
- [26] F. Fogolari and J. M. Briggs. On the variational approach to poisson-boltzmann free energies. *Chemical Physics Letters*, 281(1):135–139, 1997.
- [27] F. Fogolari, A. Brigo, and H. Molinari. The Poisson-Boltzmann equation for biomolecular electrostatics: a tool for structural biology. *Journal of Molecular Recognition*, 15(6):377–92, 2002.
- [28] D. Gilbarg and N. S. Trudinger. *Elliptic partial differential equations of second order*, volume 224 of *Grundlehren der Mathematischen Wissenschaften [Fundamental Principles of Mathematical Sciences]*. Springer-Verlag, Berlin, second edition, 1983.
- [29] J. A. Grant, B. T. Pickup, M. T. Sykes, C. A. Kitchen, and A. Nicholls. The Gaussian Generalized Born model: application to small molecules. *Physical Chemistry Chemical Physics*, 9:4913–22, 2007.
- [30] P. Grochowski and J. Trylska. Continuum molecular electrostatics, salt effects and counterion binding. a review of the Poisson-Boltzmann theory and its modifications. *Biopolymers*, 89(2):93–113, 2007.
- [31] Tzyy-Leng Horng. Review and modification of entropy modeling for steric effects in the Poisson-Boltzmann equation. *Entropy*, 22(6):Paper No. 632, 15, 2020.
- [32] Mustafa Sabri Kilic, Martin Z. Bazant, and Armand Ajdari. Steric effects in the dynamics of electrolytes at large applied voltages. i. double-layer charging. *Phys. Rev. E*, 75:021502, Feb 2007.
- [33] Mustafa Sabri Kilic, Martin Z. Bazant, and Armand Ajdari. Steric effects in the dynamics of electrolytes at large applied voltages. ii. modified poisson-nernst-planck equations. *Phys. Rev. E*, 75:021503, Feb 2007.
- [34] L. A. Kuhn, M. A. Siani, M. E. Pique, C. L. Fisher, E. D. Getzoff, and J. A. Tainer. The interdependence of protein surface topography and bound water molecules revealed by surface accessibility and fractal density measures. *Journal of Molecular Biology*, 228(1):13–22, 1992.
- [35] G. Lamm. The Poisson-Boltzmann equation. In K. B. Lipkowitz, R. Larter, and T. R. Cundari, editors, *Reviews in Computational Chemistry*, pages 147–366. John Wiley and Sons, Inc., Hoboken, N.J., 2003.
- [36] J. LeCrone, Y. Shao, and G. Simonett. The surface diffusion and the Willmore flow for uniformly regular hypersurfaces. *Discrete Contin. Dyn. Syst. Ser. S*, 13(12):3503–3524, 2020.
- [37] B. Li. Minimization of electrostatic free energy and the poisson-boltzmann equation for molecular solvation with implicit solvent. *SIAM Journal on Mathematical Analysis*, 40(6):2536–2566, 2009.
- [38] B. Li and Y. Liu. Diffused solute-solvent interface with Poisson-Boltzmann electrostatics: free-energy variation and sharp-interface limit. *SIAM J. Appl. Math.*, 75(5):2072–2092, 2015.
- [39] C. Li, L. Li, J. Zhang, and E. Alexov. Highly efficient and exact method for parallelization of grid-based algorithms and its implementation in delphi. *Journal of Computational Chemistry*, 33(24):1960–1966, 2012.
- [40] L. Li, C. Li, Z. Zhang, and E. Alexov. On the dielectric “constant” of proteins: Smooth dielectric function for macromolecular modeling and its implementation in delphi. *Journal of Chemical Theory and Computation*, 9(4):2126–2136, 2013. PMID: 23585741.

- [41] D. L. Mobley, K. A. Dill, and J. D. Chodera. Treating entropy and conformational changes in implicit solvent simulations of small molecules. *The Journal of Physical Chemistry B*, 112(3):938–946, 2008. PMID: 18171044.
- [42] J. Mongan, C. Simmerling, J. A. McCammon, D. A. Case, and A. Onufriev. Generalized Born model with a simple, robust molecular volume correction. *Journal of Chemical Theory and Computation*, 3(1):159–69, 2007.
- [43] Jan Prüss and Gieri Simonett. *Moving interfaces and quasilinear parabolic evolution equations*, volume 105 of *Monographs in Mathematics*. Birkhäuser/Springer, [Cham], 2016.
- [44] K. A. Sharp and B. Honig. Calculating total electrostatic energies with the nonlinear poisson-boltzmann equation. *The Journal of Physical Chemistry*, 94(19):7684–7692, Sep 1990.
- [45] R. S. Spolar, J. H. Ha, and M. T. Record Jr. Hydrophobic effect in protein folding and other noncovalent processes involving proteins. *Proceedings of the National Academy of Sciences of the United States of America*, 86(21):8382–8385, 1989.
- [46] J. M. J. Swanson, J. Mongan, and J. A. McCammon. Limitations of atom-centered dielectric functions in implicit solvent models. *Journal of Physical Chemistry B*, 109(31):14769–72, 2005.
- [47] H. Tjong and H. X. Zhou. GBr6NL: A generalized Born method for accurately reproducing solvation energy of the nonlinear Poisson-Boltzmann equation. *Journal of Chemical Physics*, 126:195102, 2007.
- [48] J. A. Wagoner and N. A. Baker. Assessing implicit models for nonpolar mean solvation forces: the importance of dispersion and volume terms. *Proceedings of the National Academy of Sciences of the United States of America*, 103(22):8331–6, 2006.
- [49] B. Wang and G. W. Wei. Parameter optimization in differential geometry based solvation models. *The Journal of chemical physics*, 143(13):134119, 2015.
- [50] G. W. Wei. Differential geometry based multiscale models. *Bulletin of Mathematical Biology*, 72(6):1562–1622, Aug 2010.
- [51] G. W. Wei and N. A. Baker. Differential geometry-based solvation and electrolyte transport models for biomolecular modeling: a review. In *Many-Body Effects and Electrostatics in Biomolecules*, pages 435–480. Jenny Stanford Publishing, 2016.
- [52] G. W. Wei, Y. H. Sun, Y. C. Zhou, and M. Feig. Molecular multiresolution surfaces. *arXiv:math-ph/0511001v1*, pages 1 – 11, 2005.
- [53] S. Zhao. Pseudo-time-coupled nonlinear models for biomolecular surface representation and solvation analysis. *International Journal for Numerical Methods in Biomedical Engineering*, 27(12):1964–1981, 2011.
- [54] Y. Zhao, Y. Kwan, J. Che, B. Li, and J. A. McCammon. Phase-field approach to implicit solvation of biomolecules with coulomb-field approximation. *The Journal of chemical physics*, 139(2):024111, 2013.
- [55] Y. Zhou. On curvature driven rotational diffusion of proteins on membrane surfaces. *SIAM Journal on Applied Mathematics*, 80(1):359–381, 2020.